

# Differential roles of melatonin in plant-host resistance and pathogen suppression in cucurbits

Mihir Kumar Mandal<sup>1,2</sup> | Haktan Suren<sup>3</sup> | Brian Ward<sup>4</sup> | Arezue Boroujerdi<sup>5</sup> | Chandrasekar Kousik<sup>1</sup>

<sup>1</sup>USDA, ARS, U.S. Vegetable Laboratory, Charleston, SC, USA

<sup>2</sup>ORISE Participant sponsored by the U.S. Vegetable Laboratory, USDA, ARS, Charleston, SC, USA

<sup>3</sup>Department of Forest Resources and Environmental Conservation, Virginia Tech, Blacksburg, VA, USA

<sup>4</sup>Clemson University, CREC, Charleston, SC, USA

<sup>5</sup>Department of Chemistry, Claflin University, Orangeburg, SC, USA

## Correspondence

Mihir Kumar Mandal and Chandrasekar Kousik, USDA, ARS, U.S. Vegetable Laboratory, Charleston, SC, USA.  
Emails: mihir.biotech@gmail.com and shaker.kousik@ars.usda.gov

## Funding information

SCRI Vegetable Grafting grant award, Grant/Award Number: 2016-1498-08; SCRI CuCAP grant award, Grant/Award Number: 2015-51181-24285 C; ORISE

## Abstract

Since the 1950s, research on the animal neurohormone, melatonin, has focused on its multiregulatory effect on patients suffering from insomnia, cancer, and Alzheimer's disease. In plants, melatonin plays major role in plant growth and development, and is inducible in response to diverse biotic and abiotic stresses. However, studies on the direct role of melatonin in disease suppression and as a signaling molecule in host-pathogen defense mechanism are lacking. This study provides insight on the predicted biosynthetic pathway of melatonin in watermelon (*Citrullus lanatus*), and how application of melatonin, an environmental-friendly immune inducer, can boost plant immunity and suppress pathogen growth where fungicide resistance and lack of genetic resistance are major problems. We evaluated the effect of spray-applied melatonin and also transformed watermelon plants with the melatonin biosynthetic gene SNAT (serotonin N-acetyltransferase) to determine the role of melatonin in plant defense. Increased melatonin levels in plants were found to boost resistance against the foliar pathogen *Podosphaera xanthii* (powdery mildew), and the soil-borne oomycete *Phytophthora capsici* in watermelon and other cucurbits. Further, transcriptomic data on melatonin-sprayed (1 mmol/L) watermelon leaves suggest that melatonin alters the expression of genes involved in both PAMP-mediated (pathogen-associated molecular pattern) and ETI-mediated (effector-triggered immunity) defenses. Twenty-seven upregulated genes were associated with constitutive defense as well as initial priming of the melatonin-induced plant resistance response. Our results indicate that developing strategies to increase melatonin levels in specialty crops such as watermelon can lead to resistance against diverse filamentous pathogens.

## KEYWORDS

melatonin, *N*-acetylserotonin, pathogen resistance, signaling, watermelon

## 1 | INTRODUCTION

Melatonin (*N*-acetyl-5-methoxytryptamine) is a naturally occurring low molecular weight indole-based metabolite and serves as an antioxidant molecule in various plants and animals.<sup>1-7</sup> It was first isolated and reported from the bovine pineal glands.<sup>8,9</sup> In the mammalian system, melatonin

serves as a neurohormone and is endogenously synthesized from its amino acid precursor tryptophan with serotonin as one of the major intermediate molecules in its biosynthetic process.<sup>10</sup> Melatonin is released from the pineal gland and plays an important role in regulating the circadian cycle in humans.<sup>4</sup> Melatonin has been widely used in dietary supplements for patients suffering from sleep disorders, insomnia,

dementia,<sup>11</sup> for treatment of delirium,<sup>12–14</sup> Alzheimer's disease,<sup>15,16</sup> and as anticancer adjuvants for patients undergoing chemotherapy.<sup>17,18</sup> For decades, it has been considered as an exclusive animal hormone, but research has discovered that it also has regulatory functions in plants. Recent research on melatonin has been focused on its biosynthetic pathway,<sup>19–22</sup> its physiological role in plant growth and development,<sup>23–29</sup> its importance as a phytoremediative molecule,<sup>30,31</sup> and its role as a powerful antioxidant capable of scavenging reactive oxygen species (ROS) and reactive nitrogen species (RNS).<sup>2,32–35</sup> In plants, the melatonin biosynthesis takes place through the shikimate pathway with tryptophan as the precursor amino acid.<sup>19,21,22</sup> In contrast to vertebrates, there are 6 genes (tryptophan decarboxylase, TDC; tryptamine 5-hydroxylase, T5H; tryptophan 5-hydroxylase, TPH; serotonin N-acetyltransferase, SNAT; acetylserotonin methyltransferase, ASMT; and caffeic acid *O*-methyltransferase, COMT) involved in the melatonin biosynthetic process in plants. In contrast to vertebrates, tryptophan is first catalyzed into tryptamine by tryptophan decarboxylase (TDC). Tryptamine is further catalyzed into serotonin by tryptamine 5-hydroxylase (T5H). In animals, tryptophan is first catalyzed to 5-hydroxy tryptophan-by-tryptophan 5-hydroxylase (T5H/TPH). However, there is no known reported ortholog of tryptophan 5-hydroxylase in plants, but we presume an enzyme similar to tryptophan 5-hydroxylase, T5H (TPH), may be available in plants, an alternative way of melatonin biosynthesis in plants. Serotonin is *N*-acetylated by serotonin N-acetyltransferase (SNAT) to form *N*-acetylserotonin which further gets catabolized to melatonin with the help of acetylserotonin methyltransferase (ASMT); or with the help of caffeic acid *O*-methyltransferase (COMT). SNAT is the penultimate enzyme in melatonin biosynthesis pathway and believed to be the rate-limiting enzyme in the melatonin biosynthetic pathway in animals and plants. Its regulation is tightly controlled and uses acyl-CoAs to acetylate a wide range of small molecule and protein substrates.<sup>36,37</sup> In animals, its activity is regulated by cAMP-dependent phosphorylation and hence interacts with 14-3-3 proteins to prevent its proteasomal degradation.<sup>38</sup> However, its direct interaction and molecular characterization in plants are limited.

In plants, melatonin reprograms cellular functions by activating expression of defense-related genes against diverse biotic and abiotic stresses. For example, recent studies on melatonin's role in triggering plant immunity against the bacterial pathogen *Pseudomonas syringae* pv *tomato* (*pst*) DC3000 in *Arabidopsis* plants provided evidence of its role in salicylic acid-mediated plant defense signaling.<sup>39–42</sup> Characterization of *Arabidopsis* serotonin N-acetyltransferase knockout (*AtSNAT KO*) mutant plants exhibits decreased melatonin and salicylic acid levels resulting in susceptibility to an avirulent bacterial pathogen.<sup>39</sup> In addition, various pathogenesis-related (PR) PR-1 and other defensive genes get activated in

response to melatonin by modulating the levels of nitric oxide (NO) and salicylic acid (SA) in plants.<sup>43–47</sup> All these evidence support the existence of crosstalk between melatonin and various plant hormones that facilitate fine-tuning of resistance against bacterial pathogen.

However, direct role of melatonin in disease suppression and as a signaling molecule in plant defense against fungal and oomycete pathogens has not been well characterized. In this study, we investigated the direct effects of melatonin on 2 devastating fungal pathogens, *Podospheera xanthii* (powdery mildew) and *Phytophthora capsici* (Phytophthora crown rot). Both are genetically and pathogenically highly diverse pathogens<sup>48,50</sup> and are prevalent in most parts of the United States of America (USA) and can limit productivity of watermelon and other cucurbit crops.<sup>48–50</sup> Among cucurbitaceous vegetables, watermelon occupies a very important place both in terms of area and production and is a widely cultivated vegetable crop around the world.<sup>51–53</sup> It is a rich source of ions, vitamins, antioxidants, and other enriched beneficial phytochemicals suitable for human health. Both powdery mildew (PM) caused by the foliar pathogen *P. xanthii*, and fruit and crown rot caused by *P. capsici* are of major concern to the cucurbit-breeding programs because of the unavailability of suitable resistant lines with desired marketable traits.<sup>54–56</sup> Managing both PM and Phytophthora fruit rot requires costly application of fungicides. The main objective of this study focused on utilizing management approaches that can boost plant immunity and promote healthy plant growth by application of more environmental-friendly immune inducers, bioactive molecules/metabolites such as melatonin. Here, we report that the application of eco-friendly melatonin with antifungal properties would be of great importance, particularly where fungicide resistance and lack of resistant genetic material are a problem and can serve as potential source as an alternative to synthetic chemical control methods. Although one of the recent studies showed potential role of melatonin in suppression of the late blight of potato pathogen (*Phytophthora infestans*)<sup>57</sup> however, the molecular mechanism/s of resistance signaling or pathogen suppression in presence of melatonin during *P. capsici* and *P. xanthii* infection process has not been well understood. This study was designed to utilize transcriptomic, genetic, and metabolic approach, in order to better understand the molecular mechanism(s) of action of melatonin in plant defense signaling. The results and observations showed that both exogenous application and watermelon transgenic lines enriched in melatonin could boost resistance against the foliar pathogen, *P. xanthii* (powdery mildew PM) and the soil-borne oomycete *P. capsici* (PCap) in watermelon and other cucurbit crops. We further characterized the predicted pathway of melatonin biosynthesis in watermelon and possible downstream signaling components involved in the melatonin-mediated immune pathway based on comparative transcriptomic data. Transcriptomic data

on melatonin-sprayed (1 mM) watermelon leaves suggest requirement of both PAMP-mediated (pathogen-associated molecular pattern) and ETI-mediated (effector-triggered immunity) defenses. Various plant immunity genes associated with constitutive defense as well as initial priming of the melatonin were induced in response to pathogen. The key findings of this study will be useful to explore melatonin-based alternative approaches to control diverse fungal pathogens in specialty crops such as watermelon and other cucurbits where fungicide resistance and lack of resistant genetic material are of major concern.

## 2 | MATERIALS AND METHODS

### 2.1 | Plant material and growth conditions

Seeds of watermelon germplasm lines USVL531-MDR (derived from PI 494531) and USVL677-PMS (derived from PI 269677) were seeded in sterilized Metro-Mix soil (Sun Gro Horticulture, Bellevue, WA, USA) in 50 cell trays. USVL677-PMS is susceptible to *P. xanthii* and *P. capsici*, whereas USVL531-MDR is resistant to both pathogens. The trays were kept on a heated mat at 37°C for 3-4 days for uniform seed germination. Seedlings with emerging cotyledons were kept in a room at 25°C and 60%-65% RH with 16-hour photoperiod provided by equipped cool white fluorescent bulbs with light intensity of 120  $\mu\text{mol m}^{-2} \text{s}^{-1}$ . Soil was fertilized once using Scotts Peter's 20:10:20 peat lite special general fertilizer that contained 8.1% ammoniacal nitrogen and 11.9% nitrate nitrogen. Plants were irrigated using deionized or tap water. Three- to four-week-old seedlings having 1-2 true leaves were selected for melatonin treatment and RNA-seq library preparation. Three separate plants of each genotype (USVL531-MDR, USVL677-PMS) and melatonin-treated USVL677-PMS (PMS-M) were sampled for paired-end RNA-seq library preparation. The leaf samples collected from different plants with or without treatments were directly frozen in liquid nitrogen and then stored at  $-80^{\circ}\text{C}$  until RNA extraction.

### 2.2 | Total RNA extraction, RNA-seq library preparation, and Illumina sequencing

Total RNA was isolated from frozen true leaf tissues using TRIzol reagent (Invitrogen, Carlsbad, CA, USA) following manufacturer's instructions. RNA purification steps and on-column DNase digestion were performed using the QIAGEN RNeasy Mini Kit as suggested by the manufacturer's instructions (Qiagen, Hilden, Germany). RNA-seq libraries were prepared as described previously.<sup>58</sup> The quality and integrity of each library were checked with Agilent high-sensitivity DNA chips (Agilent Technologies, Santa Clara, CA, USA). Concentrations of sequencing libraries

were quantified using Qubit fluorometer and Qubit dsDNA HS assay kit (Life Technologies). Three biological replications of each genotype (USVL531-MDR, USVL677-PMS) and melatonin-treated USVL677-PMS (PMS-M) were used for 150-bp paired-end RNA-seq sequencing (Duke Center for Genomic and Computational Biology, Durham, NC, USA) with Illumina HiSeq 4000 sequencing system (Illumina, Inc., San Diego, CA, USA).

### 2.3 | RNA-seq data analysis

Preprocessing of the next-generation sequencing (NGS) data was performed using the tools on Biopieces (<http://www.biopieces.org>). Paired-end reads were interleaved to maintain their order during the pre-processing, the bad-quality reads trimmed from both ends (min Phred quality score <35, good-quality stretch length >3) and then both forward and reverse adaptor sequences removed from the reads. The remaining reads were then filtered out by length, keeping the ones having 30 or more nucleotides (for each pair). Lastly, local mean scores were calculated and reads higher than 25 were retained for the study. High-quality reads were mapped to the watermelon reference genome *Citrullus lanatus* subsp. *Vulgaris* cv. 97103 v1<sup>59</sup> using the mem algorithm from Burrows-Wheeler aligner (a.k.a bwa).<sup>60</sup> Samtools<sup>61</sup> was used to compress the (SAM) files into BAM files. The mapping rates for each library are summarized (Figure 3). Differential expression analysis was performed using edgeR<sup>62</sup> package in R<sup>63</sup> to quantify gene/transcript expression and detect novel transcripts. In summary, for differential expression analysis biological coefficients of variation (BCV) were calculated between samples and then quasi-likelihood or dispersion (fold change) around the BCV trend was estimated using glmQLFTest function in edgeR. After that, differentially expressed genes selected as both having large fold changes and consistent among the replicates. Lastly, we used FDR ratio of <0.05 to filter the most significant differentially expressed genes.

### 2.4 | Gene annotation and classification of DEGs into functional categories

The Gene Ontology (GO) classification of all the differentially expressed genes DEGs/transcripts were categorized into broader GO classes using the GO enrichment and GO gene classification tools available in the Cucurbit Genomics Database <http://cucurbitgenomics.org/pwyeenrich> and Blast2GO server (<https://www.blast2go.com/>)<sup>64</sup>. The proteins for melatonin biosynthetic pathway in watermelon were annotated based on amino acid sequence homology to the corresponding pathway genes in *Arabidopsis*, *Oryza sativa*, and *Cyanobacterium*, which were blasted against the Cucurbit Genomics Database.

## 2.5 | Pathogen growth conditions on melatonin-treated in vitro plates, fruits and leaf inoculation assays

*Phytophthora capsici* isolates collected from different regions of the USA and from different hosts were grown on unclarified V8 juice agar plates (100 mL V8 juice, 1 g CaCO<sub>3</sub>, 500 mL H<sub>2</sub>O, 1 mL Rifampicin [25 mg/mL], 200 µL Pimaricin [2.5%], and 1 mL Ampicillin [150 mg/mL]). Agar plugs (7-mm) from an actively growing colony of *P. capsici* were transferred into new V8 juice agar plates with different concentrations of melatonin (Sigma-Aldrich, Saint Louis MO, USA). After 3–4 days, mycelial growth was recorded. Zoospore release was determined by adding sterile water (1 mL) ( $\pm$ melatonin), on 7-day-old *P. capsici* culture growing on V8 plates. Plates were kept in the refrigerator for 1 hour and brought to room temperature for zoospore release and observed under microscope to count zoospores. To evaluate development of *Phytophthora* fruit rot, cucumber fruits were inoculated with a 7-mm agar plug from an actively growing colony of *P. capsici*. Inoculated fruits were kept in a Conviron plant growth chamber maintained with conditions conducive for disease development (>95% RH, 26  $\pm$  2°C). After 5 days, lesion size, pathogen growth, and intensity of sporulation were recorded for each fruit with and without melatonin treatment (1000 ppm spray). Each of these experiments was repeated at least twice, and similar results were obtained. Data from 2 experiments have been reported with 3 biological replicates in each experiment.

For leaf inoculations, 3- to 4-week-old watermelon seedlings (USVL531-MDR, USVL677-PMS and 35S-ClaSNAT1) were inoculated with the local isolate of powdery mildew pathogen, *P. xanthii*, B108ML<sup>65,66</sup> collected from watermelon plants in the greenhouse and routinely maintained in a growth chamber on “Early Prolific Straight Neck (EPSN)” squash plants. For inoculation, the seedlings were sprayed with a conidial suspension (10<sup>5</sup> conidia/mL in 0.02% Tween-20) as described before.<sup>65–67</sup> Disease severity was recorded on the same 0–10 rating scale. For detached leaf assays, fully expanded true leaves were excised and placed on water agar plates (8 g/L) amended with sucrose (6.8 g/L), mannitol (18.2 g/L) and pimaricin (400 µL/L of 2.5% aqueous solution) covered with a round sterile blue germination blotter paper (Anchor Paper, St Paul, MN, USA) with holes punched on its edges to insert the leaf petiole into the water agar. Each disposable plastic Petri plate has leaves from USVL531-MDR, USVL677-PMS, and 35S-ClaSNAT1. The leaves were spray inoculated with a conidial suspension (10<sup>5</sup> conidia/mL in 0.02% Tween-20) as described above, and the Petri plates were placed under fluorescent lights (12-h light/12-h dark) on wire shelves in the laboratory at room temperature (25  $\pm$  2°C). Data on disease severity were

collected on 0–10 scale as reported earlier. Each line had 4 replications, and the experiment was repeated 3 times.

## 2.6 | Reverse transcription (RT)-PCR analysis

To check transcript levels of watermelon *SNAT1* and *SNAT2* after *P. capsici/P. xanthii* inoculation, we performed RT-PCR on cDNA prepared from samples collected from infected tissues using SuperScript<sup>®</sup> III Reverse Transcriptase (Invitrogen) following the manufacturer's instructions. The watermelon actin sequence was used as the internal control. The following primers were employed for relative expression of SNAT1: ClaSNAT1-Cla012046-For: 5'-TACGGGCTCACTAGAGGTATC-3'; ClaSNAT1-Cla012046-Rev: 5'-CGGATTTGATAGAGTCCCAGAA G-3'; ClaSNAT2-Cla020335-For: 5'-CAGACAAGGACCTC CAATCCCCGCGG-3'; ClaSNAT2-Cla020335-Rev: 5'-TCCAGAGCAAGGCGTCCGTGTTCTC-3'; ClaActin-Cla007792-For: 5'-TCAGCAACTGGGATGATATGG-3'; ClaActin-Cla007792-Rev: 5'-TGAGAGGAGCTTCGGTAA GA-3'. The transcripts were amplified in a reaction volume of 25 µL with the following protocol: 120 seconds at 98°C followed by 25 cycles of 30 seconds at 98°C, 30 seconds at 60°C, and 30 seconds at 72°C, with 5 minutes final extension at 72°C. For qPCR analysis of DEGs, primers are listed in Table S7.

## 2.7 | Plant transformation for overexpression of watermelon SNAT

For overexpression of the *SNAT* gene, the primers for the full-length *SNAT* gene (Cla-012046) were designed based on the watermelon draft genome of 97103 and used to amplify the *SNAT* gene from USVL677-PMS and USVL531-MDR using primer sequences: ClaSNAT-012046-Fwd: 5'-CACCA TGTTGTCTCACAAACTCTTCGCCGCC-3'; Cla-SNAT-012046-Rev-NS: 5'-ATGCTTGGGTACCAGAACATG CCTTAAATTC-3'. The final PCR product was gel purified and cloned into the pENTR vector using the Gateway based pENTR<sup>™</sup>/D-TOPO<sup>®</sup> Cloning Kit (Invitrogen) following the manufacturer's instructions. The pENTR:*SNAT* gene entry vector was then recombined with the pSITE-2NB/4NB Gateway destination vector via LR recombination to form pSITE-2NB/4NB:*SNAT*. The final construct was transformed into *Agrobacterium* strain LBA4404. The *Agrobacterium* strain carrying the *SNAT* gene either from USVL677-PMS or USVL531-MDR was transformed into USVL677-PMS background as described previously.<sup>68,69</sup> Transgenic plants were confirmed using Kanamycin selection media during callusing to complete plant regeneration from cotyledon and further confirmed using Kanamycin-specific primers on genomic DNA extracted from transgenic lines.



## 2.8 | Sequence alignment and phylogenetic tree analysis

The publically available GenBank sequences (104 amino acid sequences orthologous to SNAT in plants) were subjected to phylogenetic tree analysis using the Geneious Tree Builder (<https://www.geneious.com/features/phylogenetic-tree-building/>) based on neighbor-joining consensus tree build method. Bootstrap analysis (1000 replicates) was used to validate tree topology. The analysis resulted in different cluster groups represented in different colors (see Table S6 for additional information on gene accession, % pairwise identity, % identical similarity).

## 2.9 | Trypan blue staining

The PM infected leaves were cut into small disks and kept in 12-well plates containing 2.5 mL of clearing solution (acetic acid:ethanol::1:3, v/v). The plates were sealed and placed on a rotary shaker set at 100 rpm for 12 hours. The clearing solution was removed and replaced with 2 mL of a second clearing solution (acetic acid:ethanol:glycerol::1:5:1, v/v/v). The plates were then sealed and placed on a rotary shaker (100 rpm) for 3 hours. The second clearing solution was removed and replaced with the trypan blue staining solution (0.01% trypan blue in lactoglycerol). The plates were then placed on a rotary shaker (@ 100 rpm) overnight. The staining solution was discarded, and leaf samples were rinsed with 60% glycerol (3 ×) and mounted on a clean glass slide and covered with a coverslip.

## 2.10 | Light and fluorescent microscopy

For SNAT localization studies, *Agrobacterium* strain LBA4404 containing 35s(2x)-SNAT-GFP/RFP was infiltrated transiently into *Nicotiana benthamiana*. After 48 hours, infiltrated leaves were mounted on clean glass slides and covered with a coverslip. Samples were observed with a Leica compound microscope (Leica Microsystems Inc. IL, USA <http://www.leica-microsystems.com/home>) with attached Scope LED fluorescence illuminator with GFP ( $\lambda$  470 nm) and RFP ( $\lambda$  560 nm) filters <http://www.scopeled.com/product/fluorescence.php>. Pictures were taken with mounted Lumenera Infinity 3 CCD camera attached to the microscope.

## 2.11 | Melatonin extraction and detection

Melatonin extraction and detection were carried out using methanol-chloroform-water extractions steps based on previous reports.<sup>70,71</sup> In summary, 20 mg of freeze-dried, homogenized leaf tissues was extracted using constant solvent volume of methanol:chloroform:water::2:2:1.8 ratio according to Bligh and Dryer method.<sup>72,73</sup> The freeze-dried leaf samples

were rehydrated using ice-cold methanol/water mixture. The samples were vortexed and transferred to chloroform/water mixture in glass tubes. The samples were incubated on ice for 10 minutes and centrifuged for 10 minutes at 2000 g at 4°C. The top aqueous supernatant phase was transferred into a new microcentrifuge tube, and the extract was dried using Centrivap centrifuge. The dry extract was dissolved in 5% methanol, vortexed 2-3 times. The eluted melatonin was filtered through 0.2-micron membrane filter columns and stored at -20°C prior to HPLC run. Instrumentation: HPLC analysis was carried out using the Shimadzu system (Shimadzu, Columbia, MD, USA), which consisted of a pump, an autosampler, a column compartment, and a photodiode array detector coupled with a degassing unit. Separations were carried out using the reverse phase 5  $\mu$ m C<sub>18</sub> HPLC column (4.6 × 250 mm) (Thermo Scientific, Bellefonte, PA, USA). The temperature of column and autosampler was maintained at 30 and 4°C, respectively. The mobile phase consisted of 0.1% (v/v) formic acid (Sigma-Aldrich) in HPLC-grade acetonitrile (solvent A; Fisher Scientific, NJ, USA) and 0.1% (v/v) formic acid in HPLC-grade water (solvent B). The gradient elution program was applied with a flow rate of 0.5 mL/min. Melatonin was detected at  $\lambda_{max}$  280 nm at 16.3 minutes elution time (Figure S1).

## 3 | RESULTS

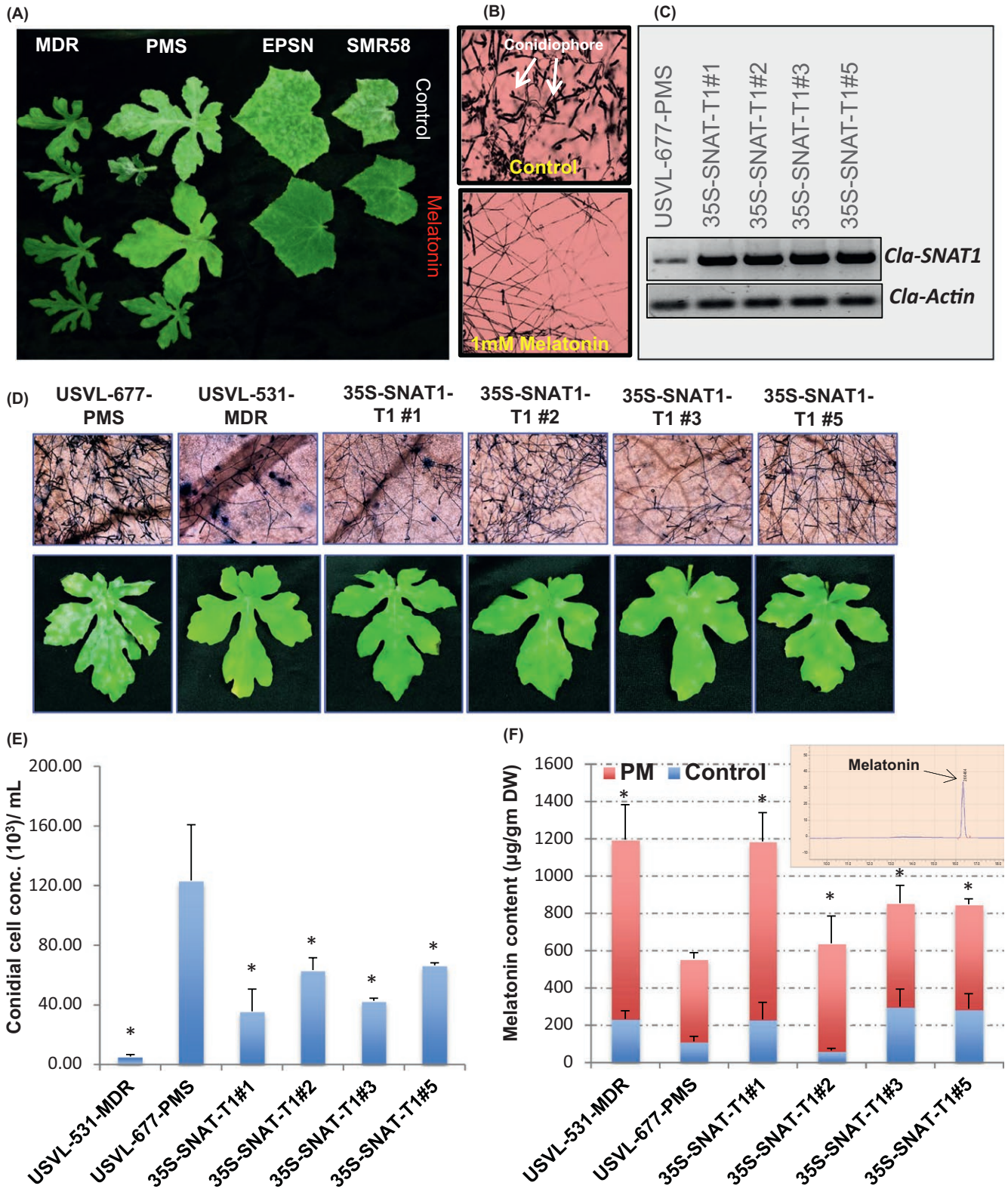
### 3.1 | Melatonin is important for systemic and basal defense against plant pathogens: *Podosphaera xanthii* and *Phytophthora capsici*

Recent evidence from our previous study has shown that melatonin is one of the mobile metabolites translocated from powdery mildew (PM)-resistant rootstocks (MDR) to susceptible watermelon scions (PMS) in grafted plants. To further test the hypothesis that if endogenous mobile melatonin has direct role in basal resistance against powdery mildew (PM) *P. xanthii*, we exogenously applied melatonin (1 mmol/L) on watermelon, zucchini and summer squash leaves and tested for powdery mildew infection. The treated leaves of watermelon, zucchini and summer squash showed a significant reduction in hyphal growth and conidia development as compared to untreated checks (Figure 1A,B), suggesting that the enhanced resistance on treated plants were due to elevated melatonin levels. Additional supporting evidence to test the hypothesis that increased melatonin levels can enhance resistance against powdery mildew was obtained by overexpressing watermelon *SNATI* with the conserved acetylase domain in PM-susceptible (USVL677-PMS) background under the control of the cauliflower mosaic virus 35S(2x) promoter and screened for resistance/susceptibility against PM pathogen. Transgenic plants overexpressing *SNATI* were morphologically similar to wild-type USVL677-PMS, and different lines

showed increased levels of the *SNAT1* transcript (Figure 1C). Detached leaf assay on PM-inoculated 35S(2x)-ClaSNAT1 transgene plants showed significant decrease in conidial count (45%-70%) and less sporulation as compared to susceptible check USVL677-PMS (Figure 1D,E), though not to the degree of the highly PM-resistant USVL531-MDR

(95%). These data indicate a role for *SNAT1* derived melatonin in regulating disease resistance against PM.

We next determined the levels of melatonin in wild-type and transgenic plants in response to PM to test the hypothesis whether the observed enhanced resistance in transgenes was due to increased melatonin levels. For a better understanding



of the role of melatonin in plant defense signaling, an in-depth analysis of its level during pathogenesis is important. Interestingly, we observed an increase in cellular melatonin levels in PM-inoculated (8DPI) USVL531-MDR, USVL677-PMS, and transgenic plants as compared to uninoculated plants (Figure 1F). We found that melatonin levels in PM-resistant line (USVL531-MDR) and one of the transgenic (35S-SNAT-T1#1) were twofold higher as compared to the PM-susceptible line, which corresponds to level of resistance against PM. In addition, the melatonin levels were monitored during early infection process and their level changes significantly within 24 hours of PM inoculation (data not shown). Together, these data provide further evidence that cellular melatonin levels changes in response to PM infection and that increased accumulation of melatonin levels is associated with increased PM resistance.

We further tested the hypothesis whether the antifungal properties of melatonin are limited to specific fungal pathogen or have broad-spectrum application and its application can be extended to another fungi/oomycetes (*P. capsici*), which is known to cause fruit rot of watermelon and other cucurbits. To test this hypothesis, we investigated the direct effect of melatonin on mycelial growth of *P. capsici* on in vitro plate experiments. Toward this objective, we evaluated the effect of melatonin (1000 ppm) on 24 *P. capsici* isolates collected from different parts of USA with diverse cucurbit host range. The minimum inhibitory concentration was 100  $\mu\text{mol/L}$ , and the mycelial growth was completely inhibited at 5–8 mmol/L for all isolates. Mycelial growth of *P. capsici* was inhibited in the range of 18%–70% of 1000 ppm melatonin after 4 days on V8 plates (Figure 2A). Melatonin significantly reduced sporulation (Figure 2B) and zoospore release of *P. capsici* (Figure 2C) at a concentration of 1000 ppm. This suggested that melatonin is capable of affecting different developmental stages of the pathogen. To further complement the in vitro data, we exogenously applied melatonin on young cucumber fruits and tested fruit rot development on inoculated with *P. capsici* (Figure 2D) at a concentration of 1000 ppm. Lesion diameter and sporulation intensity were significantly

reduced on melatonin-treated fruits as compared to the untreated check (Figure 2E). The concentration of 1000 ppm melatonin was the most effective in controlling the oomycete plant pathogen *P. capsici*. Taken together, all these results point to the broad-spectrum antifungal properties of melatonin and its potential role in affecting filamentous plant pathogens at different developmental stage of growth.

To further investigate the molecular mechanism of role of melatonin in resistance signaling during *P. capsici* infection in compatible and incompatible interaction, we inoculated resistant (USVL531-MDR) and susceptible (Charleston Grey) watermelon lines with *P. capsici*. We observed increased *SNAT* transcripts (*SNAT1* and *SNAT2*) on *P. capsici*-inoculated watermelon fruits within 2 days postinoculation (2DPI) (Figure 2F). The increased transcript levels suggest there is an increase level of cellular melatonin during pathogenesis, which could be activating the downstream plant defense pathway.

### 3.2 | Transcriptomic analysis of melatonin-treated watermelon leaves reveals activation of plant defense signaling network

To further investigate the underlying molecular mechanism(s) of role of melatonin in plant resistance signaling, we conducted genomewide gene expression profile, utilizing RNA-seq technology on watermelon leaves USVL677-PMS, treated and untreated with melatonin and compared this to a multidisease-resistant line, USVL531-MDR. For each genotype and treatment, 3 biological replicates were sequenced. Approximately 8.5 to 17 million reads were generated from each RNA-seq library with a median of 14 million reads. Most of the reads mapped (69%–94%) to the draft watermelon (*C. lanatus*, 97103) genome sequence, with transcriptome coverage in the range of 19X to 28X (Figure 3A). The expression profile analysis identified 1388 differentially expressed genes (DEGs) with 796 upregulated and 592 downregulated genes in response to melatonin treatment in USVL677-PMS (Figure 3B,C, Table S1). The DEGs between PMS-melatonin

**FIGURE 1** Melatonin effects development of powdery mildew on watermelon, summer squash, and cucumber leaves. A, Development of powdery mildew pathogen (*Podosphaera xanthii*) in the presence or absence of melatonin on foliage of watermelon, summer squash and cucumber. MDR, Powdery mildew-resistant line (USVL531-MDR); PMS, powdery mildew susceptible line (USVL677-PMS); EPSN, summer squash; SMR58: (cucumber line susceptible to PM). B, Trypan blue-stained hyphae collected from melatonin-treated and melatonin-untreated susceptible watermelon lines (USVL677-PMS) at 8 DPI with powdery mildew fungus. C, RT-PCR analysis showing levels of *SNAT1* transcripts in transgenic watermelon lines. *Actin* is used as loading control. D, Trypan blue-stained hyphae collected from susceptible watermelon line (USVL677-PMS), resistant line (USVL531-MDR), and *SNAT* overexpressed transgenic lines (T1#1, T1#2, T1#3, T1#5) at 8 DPI with powdery mildew fungus. Lower panel represents visual white powdery growth on detached leaf assay inoculated leaves of USVL677-PMS, USVL531-MDR and 35S (2x)-*SNAT*- transgenic lines at 8 DPI. E, Powdery mildew conidial development on leaves of USVL677-PMS, USVL531-MDR and 35S (2x)-*SNAT*-T1 transgenic line at 8 DPI. Asterisks indicate data statistically significant from that of control (USVL677-PMS;  $P < .05$ ). F, Melatonin levels increase in response to powdery mildew infection. Leaves of USVL677-PMS, USVL531-MDR and 35S (2x)-*SNAT*- transgenic lines were spray inoculated with *P. xanthii* conidia, and then, samples were collected at 0 hour and 8 days post inoculation for detection of melatonin using HPLC. Blue bars indicate 0 hour samples, and red bars indicate 8 DPI with PM. Asterisks indicate data statistically significant from that of control (USVL677-PMS;  $P < .05$ ). Arrow represents HPLC chromatogram of standard melatonin run elution at 16.3 minutes



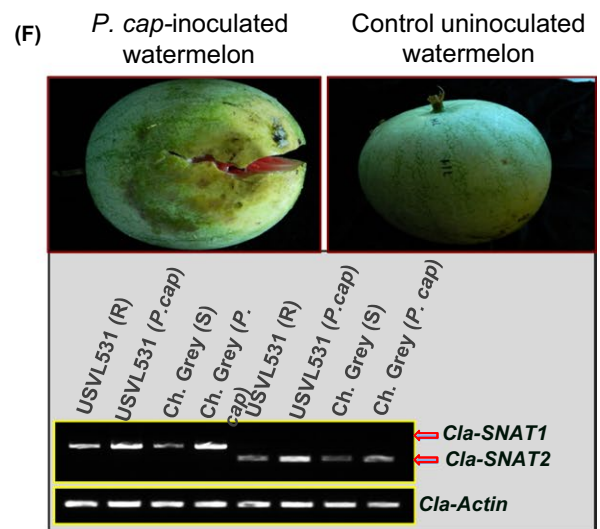
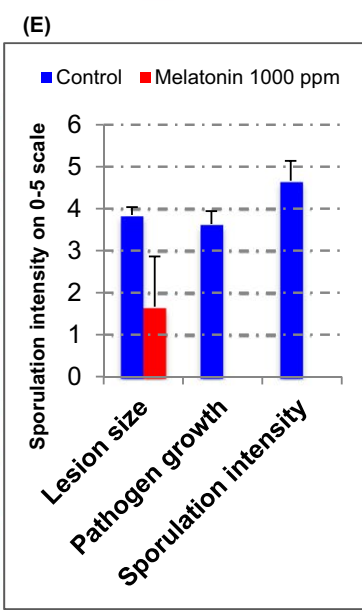
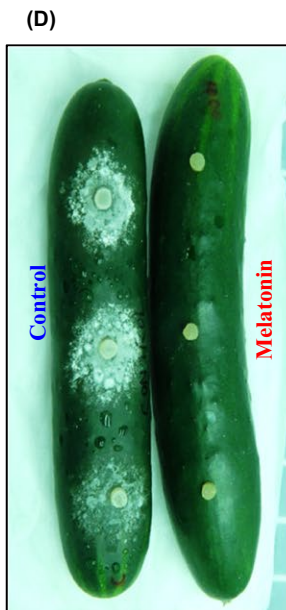
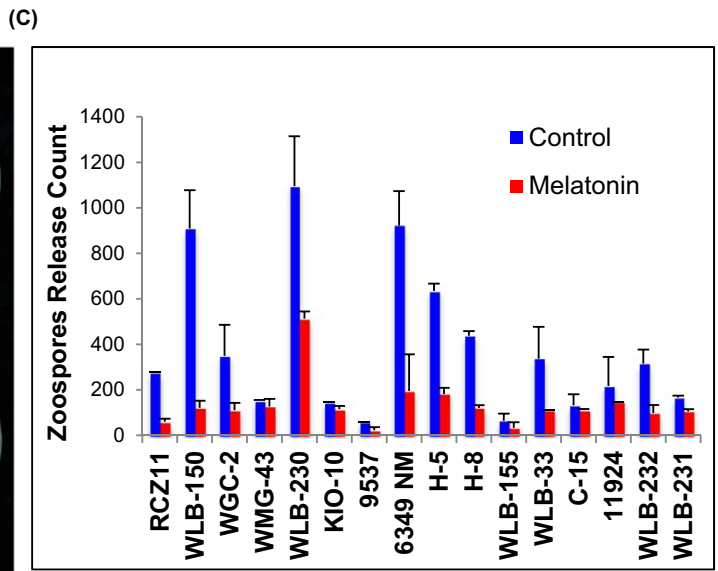
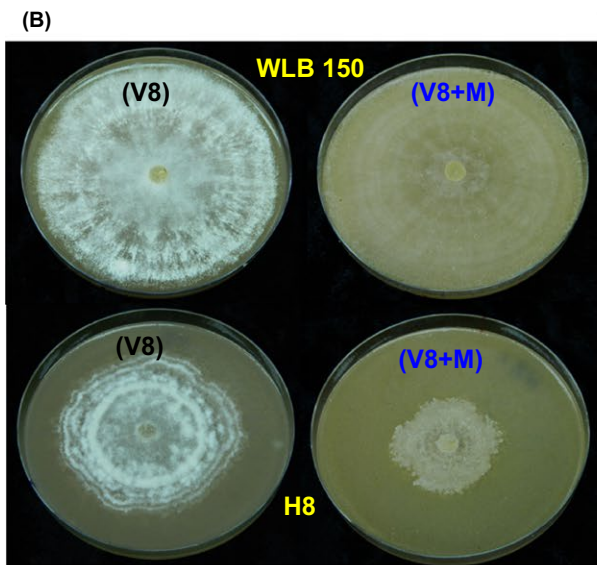
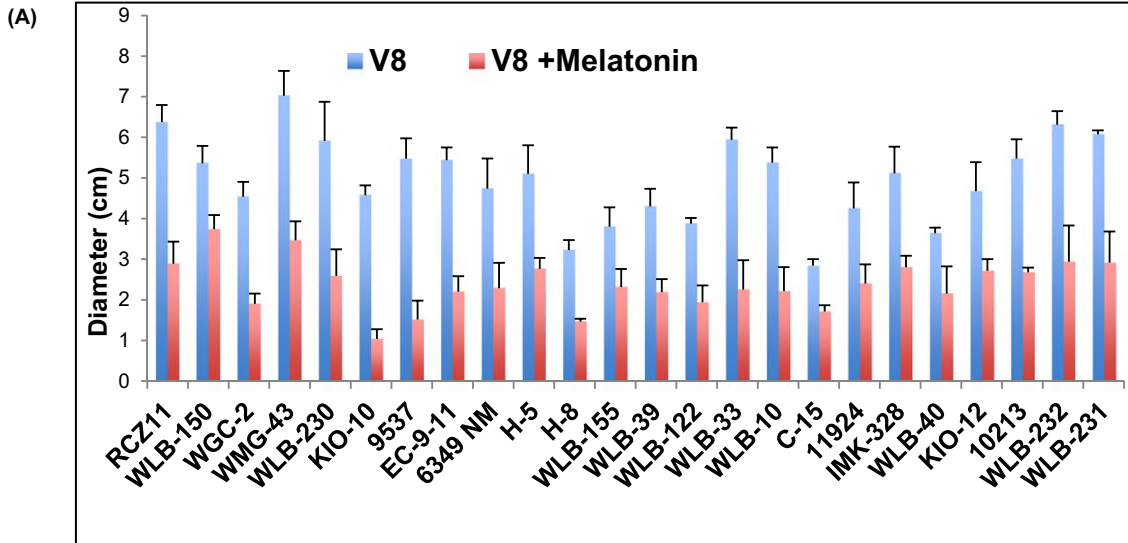




**FIGURE 2** Broad-spectrum effect of Melatonin on growth of *Phytophthora capsici*. A, Inhibition of mycelial growth *P. capsici* isolates on V8 juice agar plates amended with melatonin (1000 ppm). B, Effect of melatonin on sporulation intensity of *P. capsici* (WLB150 and H8 isolate) on V8 agar plates. V8 (- melatonin), V8 + M (+ melatonin). C, Effect of melatonin on zoospores release of *P. capsici* isolates. D, Development of *P. capsici* on cucumber, Control (- melatonin), 1000 ppm (+ melatonin). E, Effect of melatonin on lesion size, pathogen growth, and sporulation intensity in cucumber fruit inoculated with agar plug containing actively growing *P. capsici*. F, Fruit rot development on *P. capsici*-inoculated watermelon (5-7 DPI). Lower panel indicates increased transcript level of *SNAT1* and *SNAT2* genes after *P. capsici* inoculation at 2 days postinoculation (2 DPI)

and PMS treatments were grouped into GO terms based on their predicted biological process (Figure 4A), along with the number of expressed genes involved in particular biological process. Based on the expression profile analysis, melatonin treatment affects a large set of genes involved in response to biological process (1093), cellular process (916), single-organism process (817), metabolic process (810), response to stimulus (753), and developmental process (473) in plants. Interestingly, we observed that a large subgroup of genes altered by melatonin is known to be perturbed in response to plant hormones (359), providing evidence of crosstalk of melatonin with other phytohormones involved in plant defense signaling as reported earlier too with its interconnection to salicylic acid (SA), jasmonic acid (JA), ethylene (ET), and abscisic acid (ABA) regulated defense pathway. Furthermore, a large number of genes altered by melatonin were also involved in response to biotic stimulus (238)/or defense response (221), signal transduction (186) and osmotic stress (169), indicating the diverse role of melatonin in regulating plant defense signaling against biotic or abiotic conditions. As melatonin is known to detoxify free radicals and function in reduction of oxidative stress, we observed a large subset of genes involved in oxidative stress (384) providing evidence of its functional role in reactive oxygen species (ROS)-mediated signaling and a potent antioxidant molecule with its ability to nullify the adverse effects of toxic free radicals. Some of these genes were identified as members of the glutathione S-transferase (GST, 11 genes) gene family, which are involved in resistance signaling against various plant pathogens.<sup>74-77</sup>

Further analysis based on cellular components indicated that almost 30% (428) of the DE genes (DEGs) are involved in direct nuclear regulation of genes involved in biotic or abiotic stress response (Figure 4B). Most of the DEGs are involved in either selective binding (noncovalent interaction of a molecule with one or more specific sites on another molecule) and facilitate either gene regulation, modifications or involved in catalytic activities as transferases or hydrolases. Several transcription factors, receptor kinases and pathogenesis-related proteins (PR1a & PR4B) are significantly upregulated from fourfold to 16-fold in response to melatonin (Table S1). In response to melatonin, expression of several resistance proteins, both TIR-NBS-LRR and CC-NBS-LRR, was significantly changed. Taken together, our results suggest probable

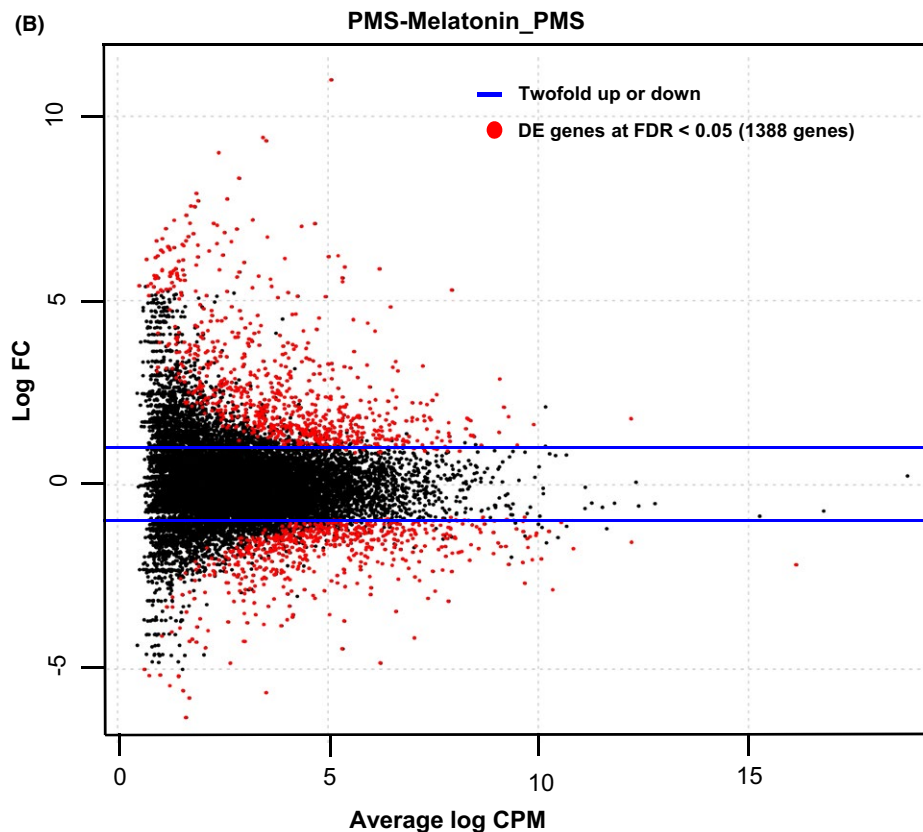
requirement of both types of resistance proteins/receptors in defense signaling induced by melatonin.

In this study, we also investigated whether the melatonin-mediated defense response overlaps with the constitutive defense response mediated by the multiple disease resistant (MDR, resistant to powdery mildew and *Phytophthora* fruit rot) watermelon USVL531-MDR by identifying common genes which are expressed both in response to melatonin treatment and are also constitutively activated in USVL531-MDR. Comparative expression analysis of transcriptome data between watermelon lines, USVL-531-MDR compared to untreated USVL-677-PMS, led to identification of 79 DEGs. Among the 79 DEGs, 37 are constitutively upregulated in USVL531-MDR compared to USVL677-PMS. Of the 37 constitutively upregulated genes, 10 genes were found to be unique to USVL531-MDR and 27 genes (Table 1) overlapped with the melatonin-mediated pathway (Figures 5A and S2). To investigate the biological function of these 27 genes, we performed gene-set enrichment analysis for biological process (Figure 5B) and cellular component (Figure 5C) analysis using Blast2Go tool, utilizing *Arabidopsis* gene annotation as a reference. Several of the genes strongly represented in response to melatonin are significantly associated with the activated defense pathway in response to external biotic stimulus (Cla021170, Cla006906, Cla007644, Cla018026, Cla016032, Cla002075, Cla001623, Cla012528, Cla015613). A number of these genes are involved in defense response to bacterial pathogen *Pseudomonas syringae* pv tomato DC3000 (Cla021170, Cla018026, Cla001623, Cla012528, Cla015613), and plant pathogenic fungi such as *P. infestans* and *Blumeria graminis* f.sp. *hordei* (powdery mildew)<sup>77,78</sup> (Cla006906, Cla018026, Cla002075, Cla015613). Two of the DEGs, Cla021170 and Cla001623, are orthologs of genes required for incompatible interaction against plant pathogens in *Arabidopsis*.<sup>79,80</sup> We also identified 4 genes (Cla021170, Cla002982, Cla012528, and Cla001623) that were strongly associated with innate immune response, which can directly recognize components of potential pathogens (MAMP/PAMP/effectors), suggesting a possible priming role in defense pathway. The upregulated genes (Cla021170, Cla018126, Cla018026, Cla002075, Cla001623), which are known to be activated in response to salicylic acid, support previous research, indicating that the defense pathway initiated by melatonin is dependent on

(A)

Sl no.	Sample	Clean reads	Mapped reads	% Mapped	Total bases	Mapped bases	Transcriptome coverage
1	PMS-1	8504361	7949107	93.5	1094653472	1033601867	23x
2	PMS-2	14947675	14074258	94.2	1923446870	1830020515	23.2x
3	PMS-3	13463772	11544661	85.7	1649858042	1457778510	28.4x
4	PMS-Melatonin-1	17737255	14777783	83.3	2231756919	1959395143	20.9x
5	PMS-Melatonin-2	13796760	12211377	88.5	1762984026	1614095409	19.9x
6	PMS-Melatonin-3	16668552	11500238	69	1998233074	1533392309	19x
7	MDR-1	19970535	16145096	80.8	2431845662	2082537450	22.7x
8	MDR-2	14476747	12955657	89.5	1808568079	1666220249	23.7x
9	MDR-3	13787670	13046245	94.6	1760729166	1684276402	23.2x

(B)



(C)

Experiment	Total DE genes	Up	Dn
PMS-Melatonin/PMS	1388	796	592

**FIGURE 3** Processed RNA-seq data. A, Total number of clean, mapped reads (watermelon), and bases of each mRNAseq sample following PM inoculation and melatonin treatments. B, Distribution of differentially expressed genes (DEGs) after exogenously applied melatonin (1 mmol/L). The DEGs are shown in red  $\log_{2}FC > 1$ ,  $P$ -value  $< .05$  and FDR ratio of  $< 0.05$  for each gene in each pairwise comparison of PMS-Melatonin and PMS (control) samples. The red dots highlight transcripts of positive and negative values of  $\log_{2}$  fold change ( $\log_{2}FC$ ), indicating that the sequences were upregulated and downregulated after melatonin treatment. The black dots indicate nondifferentially expressed genes. The genes names, fold changes, and  $P$  values, FDR values for up- and downregulated DEGs after melatonin treatment were listed in Table S1. C, The table chart indicates the total DEGs (1388) in response to melatonin, among them 796 were upregulated and 592 downregulated.

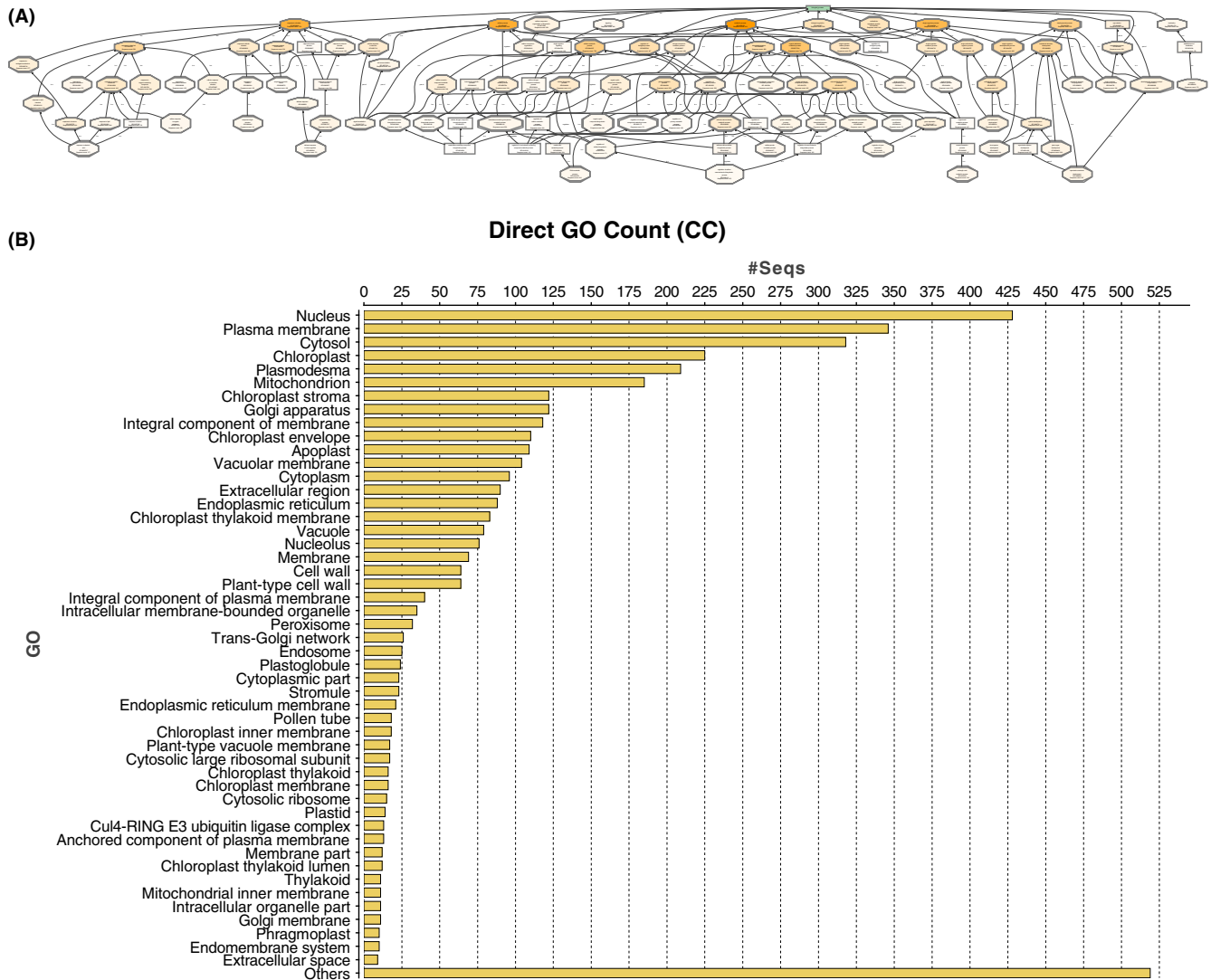


**FIGURE 4** Gene ontology classification. A, Gene ontology (GO) biological process classification of 1388 DEGs in response to 1 mmol/L melatonin treatment. B, Gene ontology (GO) cellular component classification of 1388 DEGs in response to 1 mmol/L melatonin treatment

Salicylic acid (SA). During plant defense response against biotic or abiotic stress, the first step involves perception of signal, which involves either receptor proteins such as LRR-receptor-like kinases (LRR-RLKs), which can perceive the external stimuli through their extra-cytoplasmic LRR-domain and transmit the signal to its intracellular kinase domain which further relay the information to downstream signaling components through their phosphorylation activity. Interestingly, we identified 2 LRR-receptor-like kinases (Cla001254, Cla015613), which are induced in response to melatonin and are also constitutively activated in the resistant line (USVL531-MDR). We also identified 4 upregulated genes (Cla006906, Cla018026, Cla002075, and Cla015613), which were previously known to be involved in defense response to fungi. Taken together, the expression of genes related to plant defense, including upstream and downstream signaling components mediated by activated WRKY transcription factors (Cla018026, Cla021170, Cla006906), genes

involved in redox pathways (Cla012528, Cla018162), and cell wall-associated genes (Cla003319) suggest that melatonin plays an important role in innate plant defense against biotic and abiotic stresses, presumably including foliar pathogen, *P. xanthii*, and the fruit rot pathogen, *P. capsici*.

In summary, the transcriptome data showed diverse cellular and metabolic processes were affected by melatonin, which plays an important role in induced and plant innate immunity against diverse fungal pathogens.

### 3.3 | The melatonin-mediated defense response in watermelon requires chloroplastic SNAT (<sup>Chl</sup>Cla-SNAT)

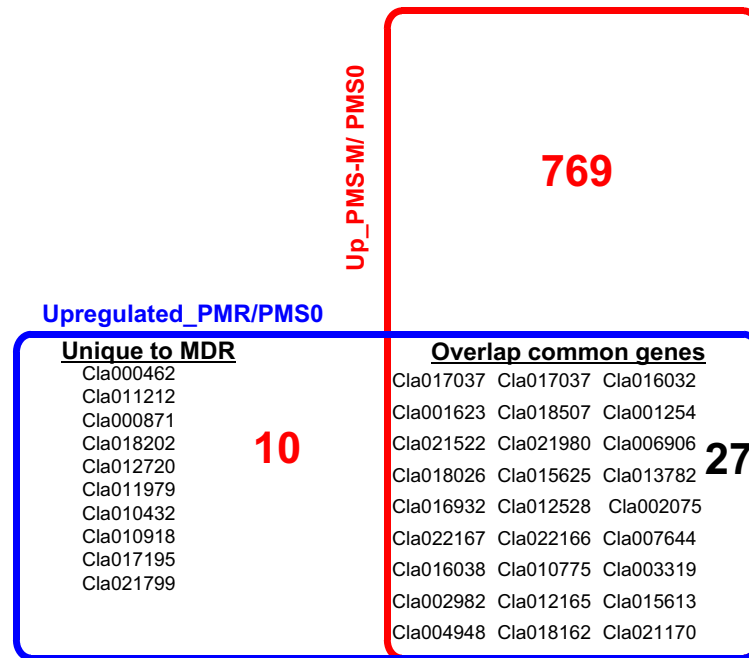
With the advancement in recent studies on melatonin biosynthetic pathway in plants, new information on genes involved in melatonin biosynthetic process has been uncovered. Both animals and plants require tryptophan as



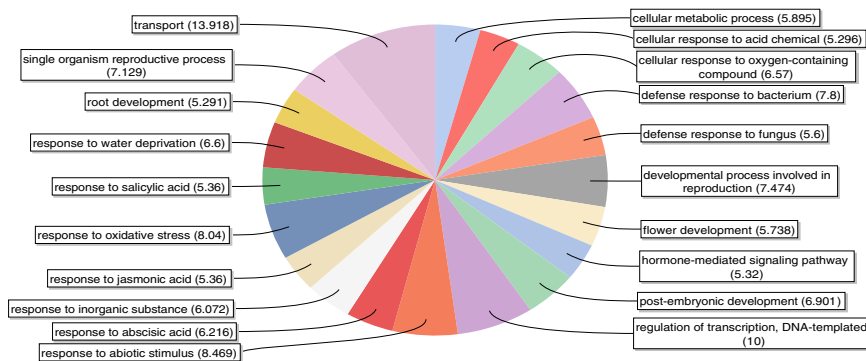
**TABLE 1** Common genes (27) constitutively upregulated in MDR and induced under 1 mmol/L exogenously applied melatonin

Geneid	Biological functions	Melatonin			USVL531-MDR				
		logFC	logCPM	PValue	FDR	logFC	logCPM	PValue	FDR
Cla017037	ATP binding/ATPase/nucleoside-triphosphatase/nucleotide-binding protein	5.30827	7.963417	4.43E-16	8.88E-13	1.776225	7.963417	0.000112	0.02633
Cla017036	ATP binding/ATPase/nucleoside-triphosphatase/nucleotide-binding protein	5.881394	6.245501	6.69E-15	1.17E-11	2.397377	6.245501	0.000126	0.028127
Cla016032	UDP glycosyltransferase	4.847446	6.505169	4.48E-14	5.73E-11	2.080837	6.505169	7.77E-05	0.021002
Cla001623	Pathogenesis-related protein 1a	6.240329	5.260622	9.83E-14	1.15E-10	3.234355	5.260622	1.30E-05	0.005939
Cla018507	Unknown Protein	3.639524	5.638188	7.19E-11	2.97E-08	1.887951	5.638188	0.000229	0.043551
Cla001254	Receptor kinase, Serine/threonine protein kinase	4.197472	4.433569	6.11E-09	1.28E-06	2.770631	4.433569	0.000256	0.046601
Cla021522	Phosphate transporter/Phosphate permease	3.42879	4.574047	2.71E-08	4.33E-06	2.249274	4.574047	0.000228	0.043551
Cla021980	Ankyrin repeat-containing protein, Zinc finger, FYVE/PHD-type	3.197156	5.547948	3.26E-08	4.90E-06	2.303803	5.547948	5.21E-05	0.016252
Cla006906	NAC domain protein, No apical meristem (NAM) protein	2.328731	6.1506	4.16E-08	6.09E-06	2.164265	6.1506	2.42E-07	0.000309
Cla018026	WRKY transcription factor 17	3.389277	4.666837	1.08E-07	1.30E-05	2.803259	4.666837	1.25E-05	0.005939
Cla015625	Auxin induced-like protein	5.366906	3.225008	2.60E-07	2.63E-05	4.575943	3.225008	3.16E-05	0.011398
Cla013782	30S ribosomal protein S13	3.581733	4.006736	4.86E-07	4.40E-05	2.738242	4.006736	0.0001	0.023881
Cla016932	Jasmonate-induced protein	4.239782	4.748954	5.31E-07	4.75E-05	4.126288	4.748954	1.42E-06	0.001104
Cla012528	Cytochrome P450	7.03483	4.390417	1.08E-06	8.51E-05	6.713013	4.390417	7.57E-06	0.004253
Cla002075	Glutaredoxin/Glutaredoxin-like, plant II	2.918313	3.330429	1.79E-06	0.00013	2.373648	3.330429	0.000114	0.026344
Cla022167	Mitochondrial carrier family, Mitochondrial substrate carrier	3.811424	3.383864	2.46E-06	0.00017	3.270392	3.383864	8.58E-05	0.021149
Cla022166	Mitochondrial carrier family, Mitochondrial substrate carrier	3.913491	3.214515	5.50E-06	0.0003	3.405707	3.214515	0.000134	0.029065
Cla007644	Ammonium transporter	1.988152	5.322446	1.14E-05	0.00054	1.731722	5.322446	0.000126	0.028127
Cla016038	Elicitor-responsive protein 3/C2 membrane targeting protein	4.167693	2.744187	4.64E-05	0.00163	3.924631	2.744187	0.000199	0.039904
Cla010775	Lipid transfer protein	2.361487	4.772964	5.62E-05	0.00187	2.497457	4.772964	2.53E-05	0.009873
Cla003319	Cellulose synthase	2.483004	3.844992	6.56E-05	0.0021	2.482811	3.844992	8.55E-05	0.021149
Cla002982	Peptidyl-prolyl cis-trans isomerase, Peptidyl-prolyl cis-trans isomerase, cyclophilin-type	1.50399	4.693251	0.000217	0.0052	1.628096	4.693251	8.31E-05	0.021149
Cla012165	Calmodulin 2, EF-Hand type	1.529167	5.072078	0.000247	0.00577	1.539218	5.072078	0.000259	0.046601
Cla015613	Receptor-like protein kinase, Serine/threonine protein kinase	1.608261	5.31499	0.000565	0.01051	1.971771	5.31499	3.69E-05	0.012971
Cla004948	Subtilisin-like serine protease, Peptidase S8, subtilisin-related	2.027128	3.526267	0.000829	0.0139	2.433023	3.526267	6.83E-05	0.018822
Cla018162	Glutathione S-transferase, C-terminal	2.263564	4.203	0.002175	0.02777	2.93845	4.203	6.00E-05	0.017308
Cla021170	WRKY transcription factor 6	1.261371	5.04771	0.002674	0.03235	2.624416	5.04771	1.30E-08	2.28E-05

(A) Gene ontology classification of overlapped common genes (27)



(B) Score Distribution (Filtered by Node Score: Cutoff = 5.0) [Biological Process]



(C) Score Distribution (Filtered by Node Score: Cutoff = 5.0) [Cellular Component]

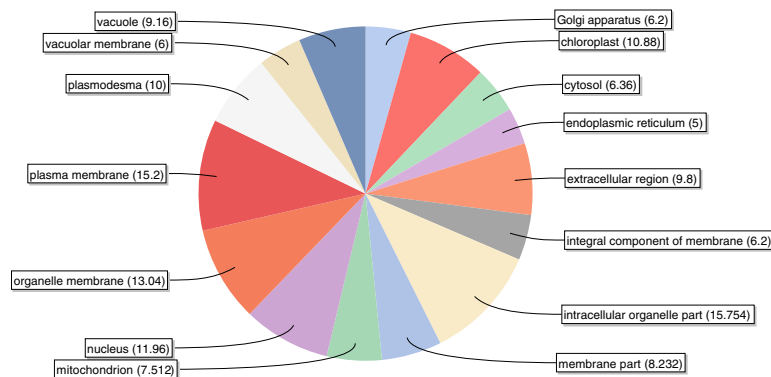
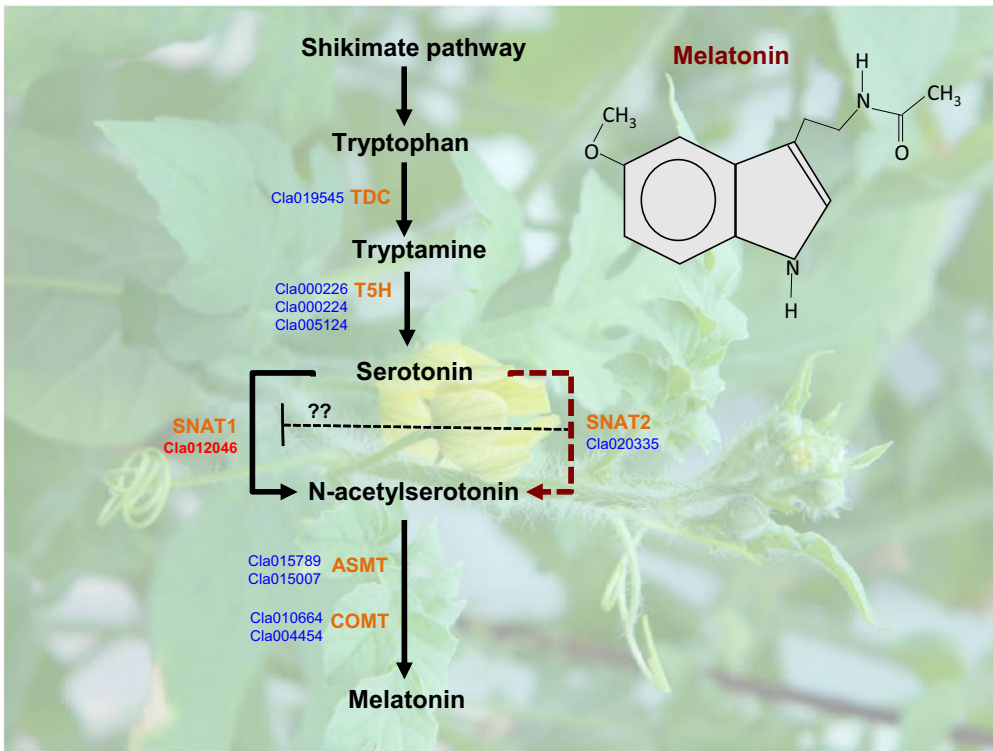
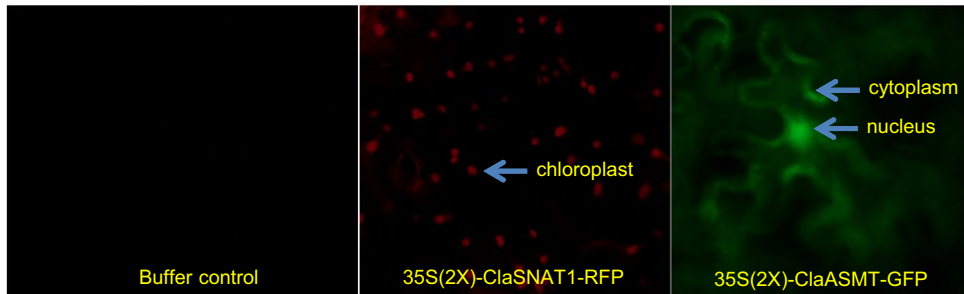


**FIGURE 5** Gene ontology classification of overlapped common genes (27). A, Venn graph representing unique and common genes upregulated in USVL531-MDR and in response to 1 mmol/L melatonin treatment. B, Pie chart showing gene ontology (GO) biological process classification of common genes (27) constitutively upregulated in MDR and induced under 1 mmol/L exogenously applied melatonin. C, Pie chart showing gene ontology (GO) cellular component classification of common genes (27) constitutively upregulated in MDR and induced under 1 mmol/L exogenously applied melatonin

(A) Predicted biosynthetic pathway of melatonin in watermelon



(B) Subcellular localization of watermelon SNAT1 and ASMT in *Nicotiana benthamiana*



(C) Phylogenetic tree view of watermelon SNAT1 and SNAT2

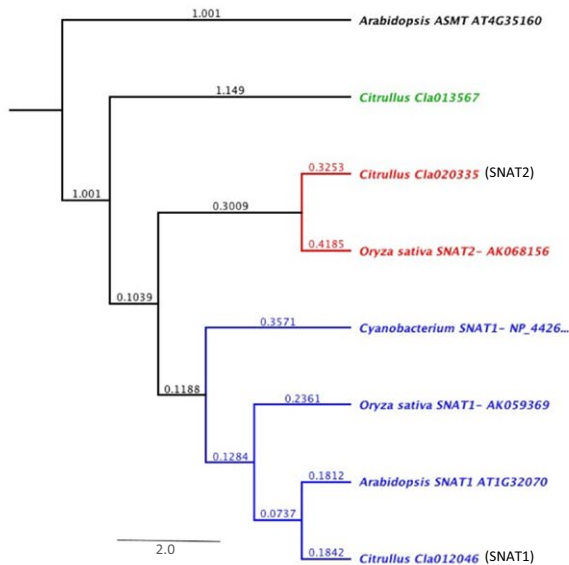




**FIGURE 6** A, Predicted Biosynthetic Pathway of Melatonin in Watermelon. The biosynthesis of melatonin (*N*-acetyl-5-methoxytryptamine) in plants requires the Shikimate pathway with tryptophan as precursor amino acid. Tryptophan is converted to tryptamine with the help of tryptophan decarboxylase (TDC; Cla019545). Tryptamine is further catalyzed into serotonin by tryptamine 5-hydroxylase (T5H, Cla00226, Cla000224, Cla005124). Serotonin is *N*-acetylated by serotonin *N*-acetyltransferase (SNAT; Cla012046) to form *N*-acetylserotonin which further gets catabolized to melatonin with the help of acetylserotonin methyltransferase (ASMT; Cla015789, Cla015007); or with the help of caffeic acid *O*-methyltransferase (COMT; Cla010664, Cla004454). Serotonin can also be *N*-acetylated by serotonin *N*-acetyltransferase2 (SNAT2; Cla020335) to form *N*-acetylserotonin. Dashed black arrow indicates possible inhibition of SNAT1 when SNAT2 is functional in melatonin biosynthesis. B, Subcellular localization of watermelon SNAT1 and ASMT in *Nicotiana benthamiana*. C, Phylogenetic tree view of watermelon SNAT1 and SNAT2. Phylogenetic relationship of SNAT1 and predicted SNAT2 proteins in watermelon, *Oryza sativa* and *Arabidopsis*. Phylogenetic relationships were inferred using neighbor-joining method. *Arabidopsis* ASMT was used as an outlier. Different cluster groups are represented in different colors (see Table S3 for additional information on gene accession, gene description, sequence length, % pairwise identity and sequence similarity). Cla indicates gene IDs of *Citrullus lanatus* 97103 cultivar

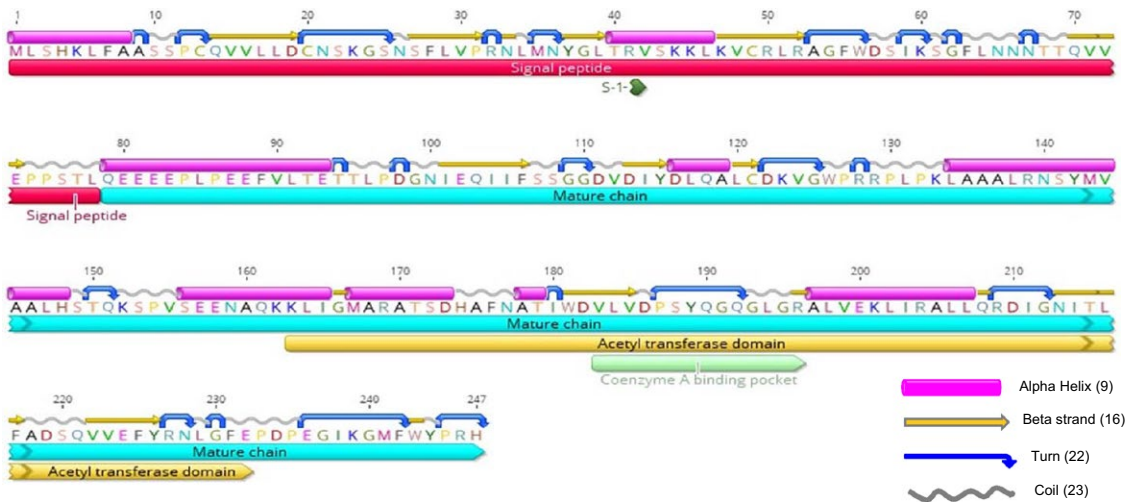
the precursor amino acid. The first 2 initial steps: hydroxylation, T5H, and decarboxylation, TDC (tryptophan-serotonin), are reversed in plants relative to animals while the last 2 steps seem to be conserved. To investigate the biosynthetic pathway utilized during melatonin biosynthesis in watermelon, we utilized the watermelon draft genome sequence ([www.icugi.org/pub/genome/watermelon/97103/v1/](http://www.icugi.org/pub/genome/watermelon/97103/v1/)) to identify similar known candidate genes involved in the melatonin biosynthetic pathway in other plants such as *Arabidopsis thaliana* and *Oryza sativa*. Based on comparative analysis of gene sequences, we identified candidate melatonin pathway genes in watermelon and its biosynthesis requires shikimate pathway with tryptophan as the precursor amino acid similar to animals. However, in contrast to animals, tryptophan is first catalyzed into tryptamine by tryptophan decarboxylase (TDC; Cla019545), which further gets metabolized into serotonin by tryptamine 5-hydroxylase ([T5H; Cla000226, Cla000224, Cla005124], Figure 6A). Serotonin is *N*-acetylated further by serotonin *N*-acetyltransferase (SNAT; Cla012046) to form *N*-acetylserotonin, which gets catabolized to melatonin with the help of acetylserotonin methyltransferase (ASMT; Cla015789, Cla015007); or with the help of caffeic acid *O*-methyltransferase (COMT; Cla010664, Cla004454). Through BLAST comparisons we identified most of the predicted orthologous gene(s) in cucurbits corresponding to the melatonin biosynthetic pathway based on sequence similarity, providing evidence of similarity in the biosynthetic pathway in most cucurbit crops (Table S2).

Previous report indicated that melatonin biosynthesis could take place in either the cytoplasm or chloroplast depending on the availability of the rate-limiting enzymes ASMT/COMT and SNAT. In order to test the subcellular source of increased accumulation of melatonin in response to pathogen defense, we dissected the melatonin biosynthetic pathway in watermelon. Full-length *SNAT1* and *ASMT* complementary DNA (cDNAs) from watermelon PI lines (USVL677-PMS, PMS: PM susceptible

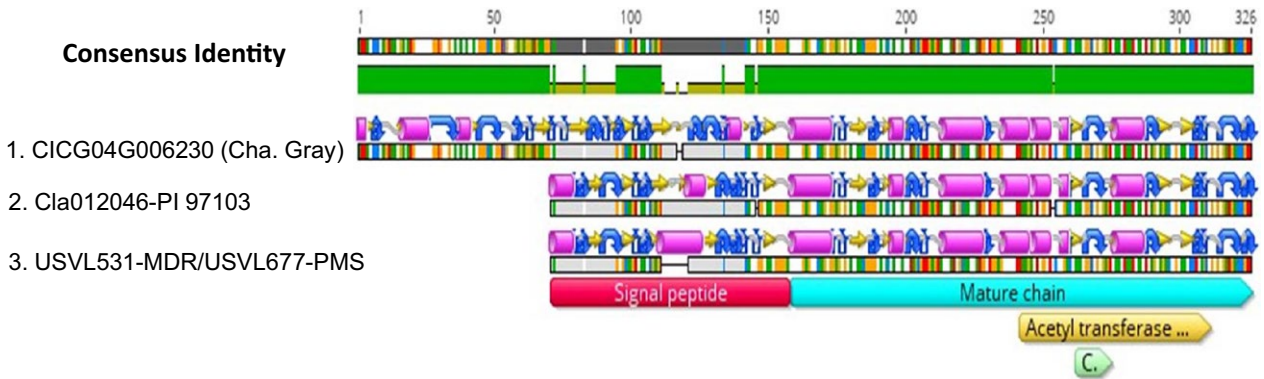
and USVL531-MDR, MDR: PM resistant) were amplified and fused upstream to GFP- or RFP-tagged reporter in pSITE-2NB/4NB vector(s). The agrobacterium strain (LBA4404) containing 35S (2x)-Cla-SNAT1-RFP and 35S (2x)-Cla-ASMT-GFP was infiltrated into *Nicotiana benthamiana*. Upon fluorescent microscopy, Cla-SNAT-RFP was found to localize to chloroplasts, whereas Cla-ASMT-GFP localized to the cytoplasm and nucleus (Figure 6B). These results suggest that there is subcellular exchange/flow of melatonin intermediates between cytoplasm and chloroplast during melatonin biosynthesis in watermelon. The subcellular localization of Cla-ASMT-GFP into nucleus and cytoplasm suggests that melatonin likely shuttles in and out of the nucleus and might be directly involved in regulating nuclear gene expressions.

Recent studies on *Arabidopsis* *SNAT* knockout mutants and rice *SNAT* RNAi lines indicated the presence/biosynthesis of melatonin in these plants in spite of either complete loss or suppression of SNAT1 functions.<sup>81</sup> It was reported that another distantly related SNAT-like protein, SNAT2 (OsSNAT2), functions independently in melatonin biosynthesis in these plants, which suggests the possibility of an alternative pathway of melatonin biosynthesis in watermelon also. We examined the presence of sequence similarity to SNAT2 like proteins in watermelon by searching the watermelon draft genome sequence [www.icugi.org/pub/genome/watermelon/97103/v1/](http://www.icugi.org/pub/genome/watermelon/97103/v1/) downloaded from the Cucurbit Genomics Database. We identified Cla020335 sequences to be phylogenetically closer to rice OsSNAT2 with 72.2% amino acid sequence similarity and 46.5% sequence identity (Table S3), suggesting its requirement in melatonin biosynthesis in addition to Cla012046 (SNAT1) (Figure 6C). The purpose of 2 SNAT isoforms could be that melatonin levels change in plants upon various stress responses (biotic and abiotic) and the influx of melatonin from either of these 2 pathways would determine a steady state of melatonin under different stress conditions.

(A) Predicted Secondary Structure of watermelon SNAT1



(B) Predicted secondary structure alignment of SNAT1 encoding protein in various watermelon cultivars



(C) Heatmap showing percentage amino acid similarity and identity between SNAT1s in different watermelon lines

% Sequence Similarity / % Sequence Identity	C1CG04G006230 (Cha. Gray)	Cla012046-PI:97103	USVL531-PMR/USVL677-PMS
C1CG04G006230 (Cha. Gray)		84.3 / 80.1%	84.3 / 80.4%
Cla012046-PI:97103	85.2 / 80.1%		95.7 / 95.7%
USVL531-MDR/USVL677-PMS	84.3 / 80.4%	95.7 / 95.7%	

**FIGURE 7** A, Predicted Secondary Structure of watermelon SNAT1. Open reading frame of SNAT1 protein with predicted secondary structure and transmembrane domains using EMBOSS 6.5.7 (Geneious software v10.2.3). Predicted secondary structures of alpha helix, beta strand, coil and turn are presented in purple cylinders, yellow arrows, gray sinusoids, and blue curved arrow. Detailed information of individual sequences is presented in Table S4. B, Amino acid consensus sequences with predicted secondary structure alignment of SNAT encoding protein in various watermelon cultivars: Charleston gray (C1CG04G006230), 97103 (Cla012046), USVL677-PMS, and USVL531-MDR. Detailed information of individual sequences is presented in Table S4. C, Heatmap showing amino acid sequence identity and similarity between SNAT1s in different watermelon lines: Charleston gray (C1CG04G006230), 97103 (Cla012046), USVL677-PMS, and USVL531-MDR

### 3.4 | *SNAT*-encoded serotonin N-acetyltransferase domain is conserved across watermelon varieties and other plant species

The *SNAT* protein has been well characterized in animals and yeast; however, in plants, the structural and functional characterization of this protein is lacking. To have a better understanding of the structures, functions, and evolution of *SNATs* across plant species, we did comparative analysis of the *SNAT* sequences obtained from different plant species. Like *Arabidopsis*, the watermelon *SNAT* consists of a N-terminal signal/transit peptide ([1-78 AA] Figure 7A), targeted to chloroplast as confirmed by our experimental subcellular localization studies and also based on information obtained from EMBOSS 6.5.7 tool, sigcleave <http://emboss.bioinformatics.nl/cgi-bin/emboss/sigcleave>, and UniProtKB {ECO:0000255|PROSITE-ProRule: PRU00532} database. The *SNAT* mature protein (79-247 AA) consists of the CoenzymeA binding pocket (183-196 AA) and the highly conserved acetyltransferase domain (163-232 AA), consisting of 6-7  $\beta$  strands (166,181,196,208,213,222) and 4 alpha-helices (156,167, 178,197), which are well conserved across watermelon cultivars and different plant species (Figure 7B, Tables S4 and S5). However, Charleston Gray (CG) (Figure 7C) has an additional N-terminal sequence compared to other watermelon cultivars; 97103, USVL531-MDR and USVL677-PMS which suggests that CG-*SNAT* might have different subcellular location than chloroplast and could be regulated differently. The comparative phylogenetic tree analysis of 104 *SNAT*-like proteins (Figure 8A, Table S6) from various plant species, including known *SNAT* sequences of *Oryza sativa* (AK059369), *Arabidopsis thaliana* (AT1G32070), and *C. lanatus* (CLCG04G006230, Cla012046), indicated that the acetylase domain (163-232 AA) is highly conserved across plant species. The conserved domain across plant species indicates the ubiquitous nature of melatonin in plants with a highly conserved step (serotonin to melatonin) in evolutionary diverse organisms and is important for diverse biological functions across plant species. We also observed watermelon *SNAT* and other cucurbit *SNATs* to be structurally conserved and hence phylogenetically grouped into the same node (*Cucumis sativus*, *cucumis melo*, *C. lanatus*) together (Figure 8B). Although the *SNAT*-acetylase domain is highly conserved, the level of melatonin in these plants varies from a few picograms to nanogram per gram of fresh weight (fw) tissues.<sup>29,82</sup> The quantitative differences of melatonin in these plants could be due to tight regulation of *SNAT* activity while catalyzing serotonin to melatonin under different environmental clues.

Our study also revealed 2 alternative splice (AS) variant forms of *SNAT* in the USVL531-MDR-resistant line (Figure 8C) indicating post-transcriptional regulation of *SNATs* in watermelon. One of the processed mRNA transcripts in USVL531-MDR-*SNAT1.2* was found to have an

intron insertion in the acetylase domain region leading to premature termination codon (PTC) in the mature chain. We also identified different *SNAT* alleles between cultivated watermelons. One of the intron sequences (S1) in the signal peptide region was retained by USVL677-PMS and USVL531-MDR as compared to 97103 (Cla012046) line suggests probable differences in subcellular localization, stability, and biological function of *SNAT* between cultivars. The functional role of these type of alternative splice variant forms/alleles of *SNAT* is still unknown and requires further characterization to have a better understanding of the regulation of melatonin biosynthesis in plants and as a source of fitness to plants under adverse environmental stress.

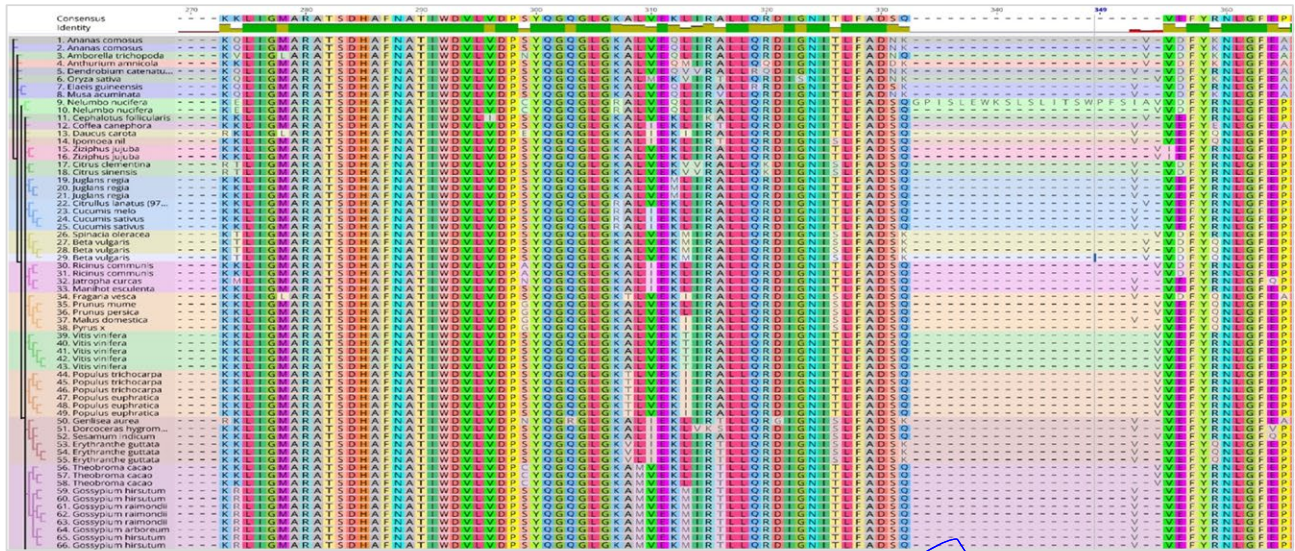
## 4 | DISCUSSION

The current study provides insight on how application of environmental-friendly immune inducer, melatonin can boost plant immunity and suppress pathogen growth (*P. xanthii* and *P. capsici*) in watermelon and other cucurbit crops, where fungicide resistance and lack of genetic resistance are of major concern. Irrespective of its known functions in animals, the function and mechanism of action of melatonin in plant defense signaling are still not fully understood. Our previous study has shown that melatonin is one of the mobile metabolites translocated from powdery mildew (PM)-resistant rootstocks (MDR) to susceptible watermelon scions (PMS) in grafted plants.<sup>70</sup> Recently, studies have also shown its role in plant immunity against *Pseudomonas syringae* pv tomato DC3000 in *Arabidopsis* and provided evidence of its involvement in plant defense and require salicylic acid (SA) as key downstream component.<sup>39-46</sup> The *Arabidopsis* serotonin N-acetyltransferase knockout (*AtSNAT KO*) mutant plants exhibit decreased melatonin and salicylic acid levels resulting in susceptibility to an avirulent bacterial pathogen. Melatonin also acts upstream with other defense signaling hormones JA, Nitric oxide (NO) and ethylene and co-regulate resistance in plants against diverse pathogens.<sup>47,82</sup> Previous reports have shown that biotic stresses involving insects/herbivores also upregulates melatonin biosynthesis in plants as a defense response.<sup>26,27,83,84</sup> However, its role as an antifungal molecule against fungal and oomycete pathogens has not been well characterized. This is the first report of the broad-spectrum role of melatonin against 2 devastating plant pathogens *P. capsici* and *P. xanthii*. Exogenous application of melatonin on in vitro V8 plates or on cucumber fruits significantly reduced *P. capsici* growth, its sporulation, and amount of zoospores released. Similarly, we observed reduced powdery mildew severity on melatonin-treated leaves of watermelon, zucchini, and summer squash, indicating its broad-spectrum antifungal activity.

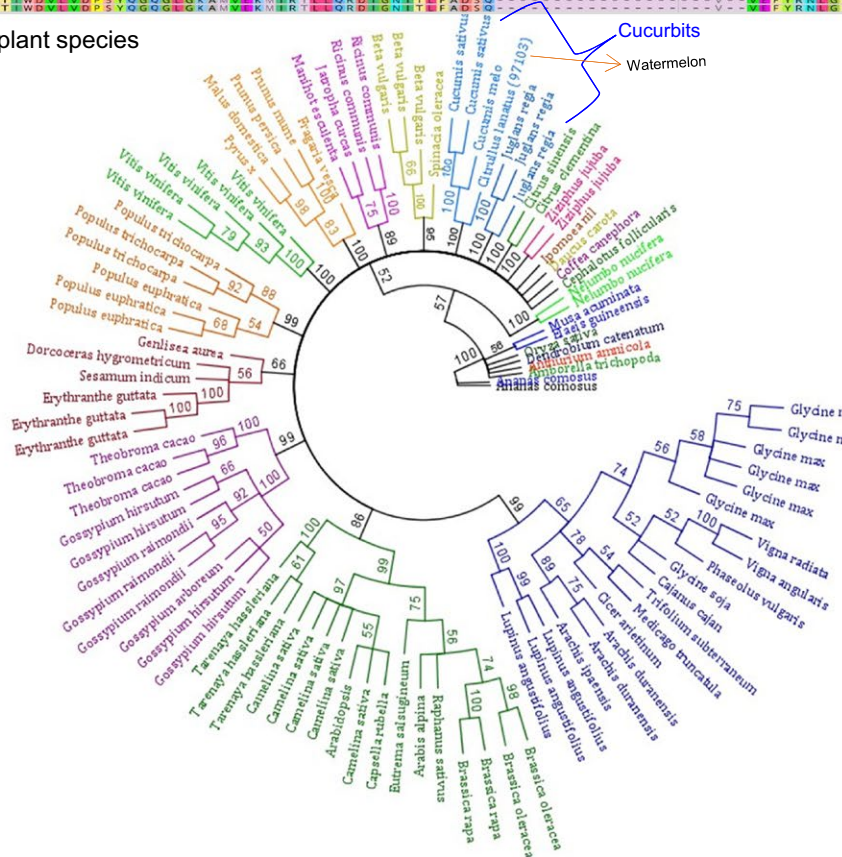
Previous studies have shown the induction of various plant defense-related genes including pathogenesis-related



(A) Conserved SNAT acetylase motif conserved across species



(B) Phylogenetic tree SNATs across plant species



(C) SNAT variants in watermelon

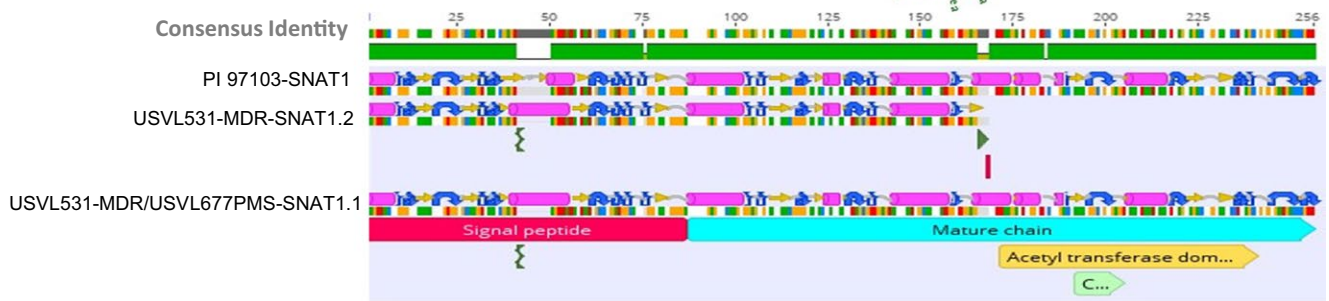


**FIGURE 8** A, Conserved SNAT-acetylase motif across plant species. Amino acid sequence alignment of conserved acetylase domain of SNAT proteins in various plant species. Detailed information of individual sequences with percentage identity and similarity is presented in Table S6. B, Phylogenetic tree analysis of SNAT proteins across plant species using publically available SNAT sequences. Phylogenetic relationships were inferred using neighbor-joining method. Bootstrap analysis (1000 replicates) was used to validate tree topology. Different cluster groups represented in different colors (see Table S5 for additional information on gene accession, gene description, sequence length, % pairwise identity, % identical sites, with heatmap matrix % sequence identity). C, SNAT1 variants in watermelon. Amino acid sequence alignment comparison of SNAT1 spliced variants in 97103 and USVL531-MDR/USVL677-PMS. S1: first spicing variant region in signal peptide, S2: second spicing variant region in mature chain (see Table S4 for additional information on gene accession, gene description, sequence length, % pairwise identity and sequence similarity)

(PR) genes in *Arabidopsis* upon exogenous application of melatonin,<sup>83</sup> which further supports its role as a plant defense signaling molecule against pathogens. Our transcriptome data analysis of melatonin-treated watermelon leaves reflected functional differences in gene expression between treated and untreated samples with increased expression of various defense-related genes involved in plant hormone signaling (SA, 35/41; JA, 18/43; ET, 14/27; ABA, 68/123 and AUX, 24/41 genes) and redox signaling (32/57 genes). Similar responses were also observed in *Arabidopsis*<sup>83</sup> in response to melatonin treatment (1 mmol/L) (SA, 70/92; JA, 53/67; ET, 32/42; ABA, 36/50 and AUX, 23/52 genes) and redox signaling (23/59 genes). Furthermore, expression of various resistance proteins along with downstream signaling cascade components (WRKY, serine/threonine kinase, MAP kinases)<sup>84-86</sup> involved in protein modifications and nuclear gene regulations were found to be altered in response to melatonin in watermelon. Several immune-related genes (27) induced by melatonin treatment were found to be constitutively expressed in the disease resistant line USVL531-MDR. These genes are known to be involved in innate plant immunity during host-pathogen interaction. High-level expression of receptor-like kinases (Cla001254 and Cla015613) are orthologs of genes known to be involved in PAMP-mediated innate immune responses in *Arabidopsis* and also function in response to oxidative stress initiated by pathogens.<sup>86,87</sup> These results provide new insights, suggesting a possible role of melatonin in plant defense signaling, from initial priming to induced plant resistance response.

Melatonin is a highly conserved bioactive molecule and ubiquitously present in evolutionary distant organisms.<sup>88-91</sup> With the availability of the draft sequence of the watermelon genome,<sup>50</sup> we were able to dissect the predicted melatonin biosynthetic pathway in watermelon evolutionary relationship of SNAT gene across species and its physiological role in plant defense signaling against powdery mildew and *Phytophthora* fruit rot. As in animals, melatonin is synthesized in watermelon from the amino acid precursor L-tryptophan with serotonin as an intermediate rate-limiting substrate for melatonin biosynthesis. Our study on localization of watermelon SNAT and ASMT proteins follows the same pattern as reported in other plant species<sup>19,92-94</sup> indicating chloroplast and

cytoplasm as the major site of its biosynthesis. Further, the presence of rice homolog of SNAT2 in sequenced genome of *C. lanatus* (97103; Cla020335) supports the possible alternate pathway of melatonin biosynthesis in watermelon in addition to SNAT1. Induced transcripts of both *SNAT1* and *SNAT2* during host-pathogen interaction reveal the requirement of both pathways contributing to host defense. We can also say that, the melatonin biosynthesis pathway is highly conserved in the cucurbits (*C. lanatus*, *cucumis sativus* L., *cucumis melo* L., *cucurbita moschata*, *cucurbita maxima*) based on the presence of predicted orthologous melatonin biosynthetic genes. These genes also share similar domain structure including a signal peptide and a highly conserved catalytic SNAT-acetylase domain within *cucurbitaceae* and across plant species. Therefore, we conclude that the melatonin biosynthetic pathway and the enzymes involved in its biosynthesis are highly conserved in cucurbits and other plant species. However, the level of melatonin in plants varies significantly depending on the stage of the plant and specific tissue in which it is synthesized.<sup>70,88,91</sup> Our recent analysis indicated significant variability in melatonin levels in commercial watermelon fruits and leaves (unpublished data). These differences in melatonin levels suggest its biosynthesis is regulated in large part by the function of the metabolite associated with the specific tissues (fruit/leaves). Importantly, our data on molecular characterization of the transgenic watermelon plants enriched in high melatonin due to overexpression of SNAT1 exhibited more tolerance to powdery mildew as compared to control susceptible check suggests the direct inhibitory effects of melatonin on growth of *P. xanthii*.

Based on our current study, we have provided new insights into the molecular mechanism(s) of defense signaling initiated by melatonin during host-pathogen interaction especially in response to fungal pathogens. We have provided a predictive model of melatonin-mediated signaling in watermelon (Figure 9). However, further, detailed analysis of some of the genes involved in melatonin-mediated defense signaling and their contribution to improved melatonin levels in plants may lead to the development of novel crops with dual functions, both enriched in antioxidant molecules and resistance to pathogens.



Proposed model illustrating melatonin regulated defense signaling in plants

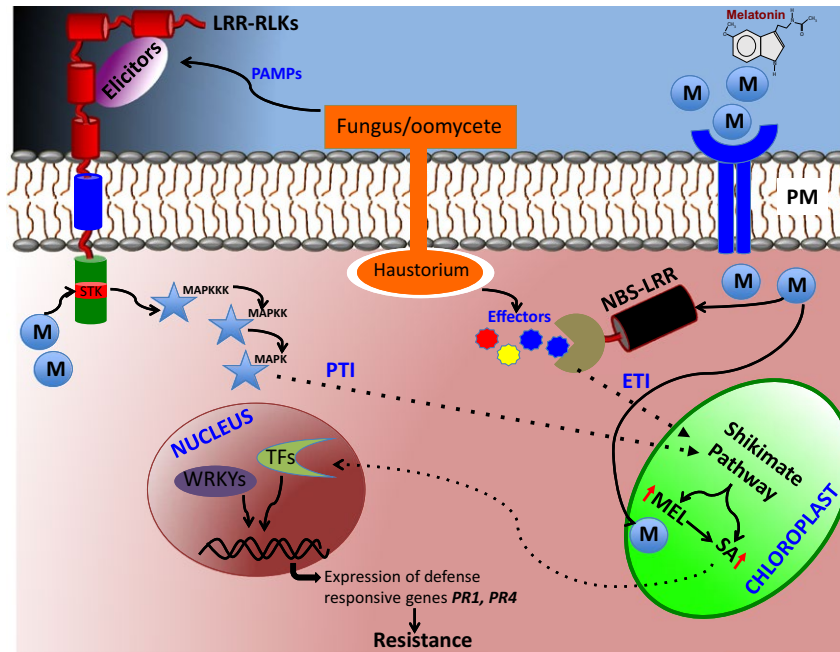


**FIGURE 9** Proposed model of melatonin-mediated signaling in watermelon. During the infection process, the plant pathogenic oomycetes and fungi develop highly specialized structures known as haustoria to secrete specific effector molecules. These effectors are recognized by the sophisticated plant-specific intracellular immune receptors (NBS-LRRs) to activate the ETI-mediated plant defense response by activating shikimate pathway to produce elevated levels of melatonin (MEL) and salicylic acid (SA) in chloroplast. The increased SA levels further potentiate downstream signaling by triggering nuclear gene expressions of various pathogenesis-related (PR1, PR4) and other defense-related genes (Table 1, Figure S2) providing resistance to pathogen. During host-pathogen interaction, these pathogenic oomycetes and fungi can also be recognized by the plasma membrane-localized host-specific receptor-like kinases (LRR-RLKs), based on their conserved PAMPs/elicitors associated with the pathogen to trigger PTI-mediated plant defense response by activating MAP kinase pathway<sup>86</sup> the shikimate pathway to produce elevated levels of melatonin (MEL) and salicylic acid (SA) in chloroplast. Exogenous application of melatonin alters expression of defense-related genes from initial perception, to downstream signaling events. Melatonin treatment can directly or indirectly activate/induce the expression of diverse intra- and extra-cellular resistance proteins require in both ETI- and PTI-mediated resistance signaling to provide resistance against the pathogenic filamentous fungi. MEL (M), melatonin; ETI, effector-triggered immunity; PAMPs, pathogen-associated molecular patterns; PTI, PAMPs triggered immunity; TFs, transcription factors; MAPKKK, map kinase kinase kinase; MAPKK, map kinase kinase; MAPK, map kinase; LRR-RLKs, leucine-rich repeat receptor-like kinases; NBS-LRR, nucleotide-binding site leucine-rich repeat

## ACKNOWLEDGEMENTS

This research was funded in part by a SCRI Vegetable Grafting grant award 2016-1498-08 and the SCRI CuCAP grant award 2015-51181-24285 to C. S. Kousik. Mihir Mandal acknowledges the fund provided by ORISE. The sequencing was performed at the Duke Center for Genomic and Computational Biology, Durham, NC, USA with Illumina HiSeq 4000 (Illumina, Inc., San Diego, CA, USA). The authors would also like to thank Dr. Amy Brunner for sharing plant transformation protocol and Jennifer Ikerd at the USVL-USDA for technical assistance in maintaining the plants in green house. The authors sincerely appreciate the critical review of the manuscript by Drs. William Rutter and Shamimuzzaman from USDA-ARS, Charleston, SC. The use of trade, firm, or corporation names in this publication is for the convenience of the reader. Such use does not constitute an official endorsement or approval by the United

States Department of Agriculture or the Agriculture Research Service of any product or service to the exclusion of others that may also be suitable.

## AUTHOR CONTRIBUTIONS

MKM and CSK conceived and directed the experiments. MKM carried out most of the experiments with help from HS in data analysis. MKM, BW, and AB did melatonin analysis. The article was prepared by CSK and MKM with contributions from all the authors.

## REFERENCES

1. Hardeland R, Madrid JA, Tan DX, Reiter RJ. Melatonin, the circadian multioscillator system and health: the need for detailed analysis of peripheral melatonin signal. *J Pineal Res.* 2012;52:139-166.

2. Hardeland R. Melatonin and the theories of aging: a critical appraisal of melatonin's role in antiaging mechanisms. *J Pineal Res.* 2013;55:325-356.
3. Hardeland R. Melatonin and circadian oscillators in aging a dynamic approach to the multiple connected players. *Interdiscip Top Gerontol.* 2015;80:128-140.
4. Buscemi N, Vandermeer B, Hooton N, et al. The efficacy and safety of exogenous melatonin for primary sleep disorders. A meta-analysis. *J Gen Intern Med.* 2005;20:1151-1158.
5. Tan DX, Hardeland R, Manchestr LC, et al. Functional roles of melatonin in plants, and perspectives in nutritional and agricultural science. *J Exp Bot.* 2012;63:577-597.
6. Tal O, Haim A, Harel O, Gerchman Y. Melatonin as an antioxidant and its semi-lunar rhythm in green macroalga *Ulva* sp. *J Exp Bot.* 2011;62:1903-1910.
7. Reiter RJ, Tan DX, Zhou Z, Cruz MHC, Fuentes-Broto L, Galano A. Phytomelatonin: assisting plants to survive and thrive. *Molecules.* 2015;20:7396-7437.
8. Lerner AB, Case JD, Takahashi Y. Isolation of melatonin, a pineal factor that lightens melanocytes. *J Am Chem Soc.* 1958;80:2587.
9. Maronde E, Stehle J. The mammalian pineal gland: known facts, unknown facets. *Trends Endocrinol Metab.* 2007;18:142-149.
10. Reiter RJ. Pineal melatonin: cell biology of its synthesis and of its physiological interactions. *Endocr Rev.* 1991;12:151-180.
11. Xu J, Wang LL, Dammer EB, et al. Melatonin for sleep disorders and cognition in dementia: a meta-analysis of randomized controlled trials. *Am J Alzheimers Dis Other Demen.* 2015;5:439-447.
12. Hanania M, Kitain E. Melatonin for treatment and prevention of postoperative delirium. *Anesth Analg.* 2002;94:338-339.
13. Hatta K, Kishi Y, Wada K, et al. DELIRIA-J Group. Preventive effects of ramelteon on delirium: a randomized placebo controlled trial. *JAMA Psychiatry.* 2014;71:397-403.
14. Al-Aama R, Brymer C, Gutmanis I, Woolmore-Goodwin SM, Esbaugh J, Dasgupta M. Melatonin decreases delirium in elderly patients: a randomized, placebo-controlled trial. *Int J Geriatr Psychiatry.* 2011;26:687-694.
15. McCleery J, Cohen DA, Sharpley AL. Pharmacotherapies for sleep disturbances in Alzheimer's disease. *Cochrane Database Syst Rev.* 2014;3:CD009178.
16. Rosales-Corral SA, Acuna-Castroviejo D, Coto-Montes A, et al. Alzheimer's diseases: pathological mechanisms and the beneficial role of melatonin. *J Pineal Res.* 2012;52:167-202.
17. Wang YM, Jin BZ, Ai F, et al. The efficacy and safety of melatonin in concurrent chemotherapy or radiotherapy for solid tumors: a meta-analysis of randomized controlled trials. *Cancer Chemother Pharmacol.* 2012;69:1213-1220.
18. Sookprasert A, Johns NP, Phunmanee A, et al. Melatonin in patients with cancer receiving chemotherapy: a randomized, double-blind, placebo-controlled trial. *Anticancer Res.* 2014;34:7327-7337.
19. Byeon Y, Lee HY, Lee K, Park S, Back K. Cellular localization and kinetics of the rice melatonin biosynthetic enzymes SNAT and ASMT. *J Pineal Res.* 2014;56:107-114.
20. Kolar J, Machackova I. Melatonin in higher plants: occurrence and possible functions. *J Pineal Res.* 2005;39:333-341.
21. Krystyna MJ, Posmyk MM, Janas KM. Melatonin in plants. *Acta Physiol Plant.* 2009;31:1-11.
22. Back K, Tan DX, Reiter RJ. Melatonin biosynthesis in plants: multiple pathways catalyze tryptophan to melatonin in the cytoplasm or chloroplasts. *J Pineal Res.* 2016;56:107-114.
23. Arnao MB, Hernández-Ruiz J. The physiological function of melatonin in plants. *Plant Signal Behav.* 2006;1:89-95.
24. Arnao MB, Hernández-Ruiz J. Chemical stress by different agents affects the melatonin content of barley roots. *J Pineal Res.* 2009;46:295-299.
25. Arnao MB, Hernández-Ruiz J. Growth conditions determine different melatonin levels in *Lupinus albus* L. *J Pineal Res.* 2013;55:149-155.
26. Arnao MB, Hernandez-Ruiz J. Melatonin: plant growth regulator and/or biostimulator during stress? *Trends Plant Sci.* 2014;19:789-797.
27. Arnao M, Hernandez-Ruiz J. Functions of melatonin in plants: a review. *J Pineal Res.* 2015;59:133-150.
28. Badria FA. Melatonin, serotonin, and tryptamine in some Egyptian food and medicinal plants. *J Med Food.* 2002;5:153-157.
29. Van-Tassel DL, Roberts N, Lewy A, O'Neil SD. Melatonin in plant organs. *J Pineal Res.* 2001;31:8-15.
30. Kolar J, Machackova I, Eder J, et al. Melatonin: occurrence and daily rhythm in *Chenopodium rubrum*. *Phytochemistry.* 1997;44:1407-1413.
31. Tan DX, Manchester LC, Helton P, Reiter RJ. Phytoremediative capacity of plants enriched with melatonin. *Plant Signal Behav.* 2007b;2:514-516.
32. Tan DX, Manchester LC, Esteban-Zubero E, Zhou Z, Reiter RJ. Melatonin as a potent and inducible endogenous antioxidant: synthesis and metabolism. *Molecules.* 2015;20:18886-18906.
33. Jiang FM, Teng FX, Zhi ZW, Yu LF, Zhu MX, Zhen WZ. The ameliorative effects of exogenous melatonin on grape cuttings under water-deficient stress: antioxidant metabolites, leaf anatomy, and chloroplast morphology. *J Pineal Res.* 2014;57:200-212.
34. Reiter RJ, Manchester LC, Tan DX. Melatonin in walnuts: influence on levels of melatonin and total antioxidant capacity of blood. *Nutrition.* 2005;21:920-924.
35. Reiter RJ, Tan DX. Melatonin: an antioxidant in edible plants. *Ann N Y Acad Sci.* 2002;957:341-344.
36. Vetting MW, S de Carvalho LP, Yu M, et al. Structure and functions of the GNAT superfamily of acetyltransferases. *Arch Biochem Biophys.* 2005;1:212-226.
37. Klein DC, Ganguly S, Coon S, et al. 14-3-3 Proteins and photoneuroendocrine transduction: role in controlling the daily rhythm in melatonin. *Biochem Soc Trans.* 2002;4:365-373.
38. Rosiak J, Zawilska JB. 14-3-3 proteins—a role in the regulation of melatonin biosynthesis. *Postepy Biochem.* 2006;1:35-41.
39. Lee HY, Byeon Y, Tan DX, Reiter RJ, Back K. Arabidopsis serotonin N-acetyltransferase knockout mutant plants exhibit decreased melatonin and salicylic acid levels resulting in susceptibility to an avirulent pathogen. *J Pineal Res.* 2015;3:291-299.
40. Lee HY, Byeon Y, Back K. Melatonin as a signal molecule triggering defense responses against pathogen attack in Arabidopsis and tobacco. *J Pineal Res.* 2014;57:262-268.
41. Qian Y, Tan DX, Reiter RJ. Comparative metabolomic analysis highlights the involvement of sugars and glycerol in melatonin-mediated innate immunity against bacterial pathogen in Arabidopsis. *Sci Rep.* 2015;5:15815.
42. Vielma JR, Bonilla E, Chacin-Bonilla L, Mora M, Medina-Leendertz S, Bravo Y. Effects of melatonin on oxidative stress,



- and resistance to bacterial, parasitic, and viral infections: a review. *Acta Trop.* 2014;137:31-38.
43. Yin L, Wang P, Li M, et al. Exogenous melatonin improves *Malus* resistance to Marssonina apple blotch. *J Pineal Res.* 2013;54:426-434.
  44. Shi H, Chen Y, Tan DX, Reiter RJ, Chan Z, He C. Melatonin induces nitric oxide and the potential mechanisms relate to innate immunity against bacterial pathogen infection in *Arabidopsis*. *J Pineal Res.* 2015;59:102-108.
  45. Zhao H, Xu L, Su T, Jiang Y, Hu L, Ma F. Melatonin regulates carbohydrate metabolism and defenses against *Pseudomonas syringae* pv. tomato DC3000 infection in *Arabidopsis thaliana*. *J Pineal Res.* 2015;59:109-119.
  46. Shi H, Wei Y, He C. Melatonin-induced CBF/DREB1s are essential for diurnal change of disease resistance and CCA1 expression in *Arabidopsis*. *Plant Physiol Biochem.* 2016;100:150-155.
  47. Mandal MK, Chandra-Shekar AC, Jeong RD, et al. Oleic acid-dependent modulation of NITRIC OXIDE ASSOCIATED 1-protein levels regulates nitric oxide-mediated signaling in plant defense. *Plant Cell.* 2012;24:1654-1674.
  48. Keinath AP, DuBose B. Evaluation of fungicides for prevention and management of powdery mildew on watermelon. *Crop Prot.* 2004;23:35-42.
  49. Lamour KH, Stam R, Jupe J, Huitema E. The oomycete broad-host-range pathogen *Phytophthora capsici*. *Mol Plant Pathol.* 2012;13:329-337.
  50. Kousik CS, Ikerd JL, Hassell RL. Effect of resistant rootstocks on development of Powdery mildew on susceptible watermelon scion, 2013. *Plant Dis Manag Rep.* 2014;8:V309.
  51. Guner N, Wehner TC. Overview of potyvirus resistance in watermelon, Proc. IXth EUCARPIA Meeting on Genetics and Breeding of Cucurbitaceae 2008; 445-451.
  52. Wechter WP, Kousik CS, McMillan ML, Levi A. Identification of resistance to *Fusarium oxysporum* f. sp. *niveum* race 2 in *Citrullus lanatus* var. *citroides* plant introductions. *HortScience.* 2012;47:334-338.
  53. Levi A, Jarret R, Kousik S, Wechter WP, Nimmakayala P, Reddy U. Genetic resources of watermelon. In: Grumet R, Katzir N, Garcia-Mas J, eds. *Genetics and Genomics of the Cucurbitaceae*. New York, NY: Springer Intl Pub AG; 2017.
  54. Davis AR, Levi A, Tetteh A, Wehner T, Russo V, Pitrat M. Evaluation of watermelon and related species for resistance to race 1W Powdery Mildew. *J Am Soc Hortic Sci.* 2007;132:790-795.
  55. Kousik CS, Ikerd J, Wechter WP, Harrison H, Levi A. Resistance to phytophthora fruit rot of watermelon caused by *Phytophthora capsici* in U.S. Plant Introductions. *HortScience.* 2012;47:1682-1689.
  56. Kousik CS, Ling KS, Adkins ST, Webster CG, Turechek W. Phytophthora fruit rot-resistant watermelon germplasm lines: USVL489-PFR, USVL782-PFR, USVL203-PFR, and USVL020-PFR. *HortScience.* 2014;49:101-104.
  57. Zhang S, Zheng X, Reiter RJ, et al. Melatonin attenuates potato late blight by disrupting cell growth, stress tolerance, fungicide susceptibility and homeostasis of gene expression in *Phytophthora infestans*. *Front Plant Sci.* 2017;8:1993.
  58. Hunt AG. A rapid, simple and inexpensive method for the preparation of strand-specific RNA-Seq libraries. *Methods Mol Biol.* 2015;1255:195-207.
  59. Guo S, Zhang J, Sun H, et al. The draft genome of watermelon (*Citrullus lanatus*) and resequencing of 20 diverse accessions. *Nat Genet.* 2013;45:51-58.
  60. Li H, Durbin R. Fast and accurate short read alignment with Burrows-Wheeler transform. *Bioinformatics.* 2009;25:1754-1760.
  61. Li H, Handsaker B, Wysoker A, et al. The Sequence alignment/map (SAM) format and SAMtools. *Bioinformatics.* 2009;25:2078-2079.
  62. Robinson MD, McCarthy DJ, Smyth GK. edgeR: a Bioconductor package for differential expression analysis of digital gene expression data. *Bioinformatics.* 2010;26:139-140.
  63. R Core Team. *R: A Language and Environment for Statistical Computing*. Vienna, Austria: R Core Team; 2017.
  64. Götz S, García-Gómez JM, Terol J, et al. High-throughput functional annotation and data mining with the Blast2GO suite. *Nucleic Acids Res.* 2008;36:3420-3435.
  65. Kousik CS, Donahoo RS, Webster CG, Turechek WW, Adkins ST, Roberts PD. Outbreak of cucurbit powdery mildew on watermelon fruit caused by *Podosphaera xanthii* in southwest Florida. *Plant Dis.* 2011;95:1586.
  66. McGrath MT. Powdery mildew. In: Keinath AP, Wintermantel WM, Zitter TA, eds. *Compendium of Cucurbit Diseases and Pests* (2nd edn). St. Paul, MN: APS Press; 2017:62-64.
  67. Kousik CS, Mandal MK, Hassell R. Powdery mildew resistant rootstocks that impart tolerance to grafted susceptible watermelon scion seedlings. *Plant Dis.* 2018. <https://apsjournals.apsnet.org/doi/pdf/10.1094/PDIS-09-17-1384-RE>.
  68. Yu TA, Chiang CH, Wu HW, et al. Generation of transgenic watermelon resistant to Zucchini yellow mosaic virus and Papaya ringspot virus type W. *Plant Cell Rep.* 2011;30:359-371.
  69. Tian S, Jiang L, Gao Q, et al. Efficient CRISPR/Cas9-based gene knockout in watermelon. *Plant Cell Rep.* 2017;36:399-406.
  70. Mahmud I, Kousik C, Hassell R, Chowdhury K, Boroujerdi AF. NMR spectroscopy identifies metabolites translocated from powdery mildew resistant rootstocks to susceptible watermelon scions. *J Agric Food Chem.* 2015;36:8083-8091.
  71. Kim HK, Choi YH, Verpoorte R. NMR-based metabolomics analysis of plants. *Nat Protoc.* 2010;5:536-549.
  72. Bligh EG, Dyer WJ. A rapid method of total lipid extraction and purification. *Can J Biochem Physiol.* 1959;37:911-917.
  73. Wu H, Southam AD, Hines A, Viant MR. High-throughput tissue extraction protocol for NMR- and MS-based metabolomics. *Anal Biochem.* 2008;372:204-212.
  74. Han Q, Chen R, Yang Y, et al. A glutathione S-transferase gene from *Lilium regale* Wilson confers transgenic tobacco resistance to *Fusarium oxysporum*. *Sci Hortic.* 2016;198:370-378.
  75. Han Y, Mhamdi A, Chaouch S, Noctor G. Regulation of basal and oxidative stress-triggered jasmonic acid-related gene expression by glutathione. *Plant, Cell Environ.* 2013;36:1135-1146.
  76. Liao W, Ji L, Wang J, et al. Identification of glutathione S-transferase genes responding to pathogen infestation in *Populus tomentosa*. *Funct Integr Genomics.* 2014;14:517-529.
  77. Collinge M, Boller T. Differential induction of two potato genes, *Stprx2* and *StNAC*, in response to infection by *Phytophthora infestans* and to wounding. *Plant Mol Biol.* 2001;46:521-529.
  78. Jensen MK, Rung JH, Gregersen PL, et al. The HvNAC6 transcription factor: a positive regulator of penetration resistance in barley and *Arabidopsis*. *Plant Mol Biol.* 2007;65:137-150.

79. Higashi K, Ishiga Y, Inagaki Y, Toyoda K, Shiraishi T, Ichinose Y. Modulation of defense signal transduction by flagellin-induced WRKY41 transcription factor in *Arabidopsis thaliana*. *Mol Genet Genomics*. 2008;279:303-312.
80. Nie P, Li X, Wang S, Guo J, Zhao H, Niu D. Induced systemic resistance against *Botrytis cinerea* by *Bacillus cereus* AR156 through a JA/ET- and NPR1-dependent signaling pathway and activates PAMP-triggered immunity in arabidopsis. *Front Plant Sci*. 2017;8:238.
81. Byeon Y, Lee HY, Back K. Cloning and characterization of the serotonin *N*-acetyltransferase-2 gene (SNAT2) in rice (*Oryza sativa*). *J Pineal Res*. 2016a;2:198-207.
82. Arnao MB, Hernández-Ruiz J. Melatonin in its relationship to plant hormones. *Ann Bot*. 2018;121:195-207.
83. Weeda S, Zhang N, Zhao X, et al. Arabidopsis transcriptome analysis reveals key roles of melatonin in plant defense systems. *PLoS ONE*. 2014;9:e93462.
84. Lee HY, Black K. Melatonin is required for H<sub>2</sub>O<sub>2</sub>- and NO-mediated defense signaling through MAPKKK3 and OXII in *Arabidopsis thaliana*. *J Pineal Res*. 2017;62:e12379.
85. Lei L, Li Y, Wang Q, et al. Activation of MKK9-MPK3/MPK6 enhances phosphate acquisition in *Arabidopsis thaliana*. *New Phytol*. 2014;4:1146-1160.
86. King SR, McLellan H, Boevink PC, et al. *Phytophthora infestans* RXLR effector PexRD2 interacts with host MAPKKK  $\epsilon$  to suppress plant immune signaling. *Plant Cell*. 2014;26:1345-1359.
87. Hardeland R. Melatonin: signaling mechanisms of a pleiotropic agent. *BioFactors*. 2009;35:183-192.
88. Chen G, Huo Y, Tan DX, Liang Z, Zhang W, Zhang Y. Melatonin in Chinese medicinal herbs. *Life Sci*. 2003;73:19-26.
89. Murch S, Campbell SSB, Saxena PK. The role of serotonin and melatonin in plant morphogenesis. Regulation of auxin-induced root organogenesis in in vitro-cultured explants of *Hypericum perforatum* L. *In vitro Cell Dev Biol Plant*. 2001;37:786-793.
90. Zhao Y, Tan DX, Lei Q, et al. Melatonin and its potential biological functions in the fruits of sweet cherry. *J Pineal Res*. 2013;55:79-88.
91. Feng X, Wang M, Zhao Y, Han P, Dai Y. Melatonin from different fruit sources, functional roles, and analytical methods. *Trends Food Sci Tech*. 2014;37:21-31.
92. Byeon Y, Lee HJ, Lee HY, Back K. Cloning and functional characterization of the Arabidopsis *N*-acetylserotonin *O*-methyltransferase responsible for melatonin synthesis. *J Pineal Res*. 2016a;1:65-73.
93. Zuo B, Zheng X, He P, et al. Overexpression of MzASMT improves melatonin production and enhances drought tolerance in transgenic *Arabidopsis thaliana* plants. *J Pineal Res*. 2014;4:408-417.
94. Tan DX, Manchester LC, Liu X, Rosales-Corral SA, Acuna-Castroviejo D, Reiter RJ. Mitochondria and chloroplasts as the original sites of melatonin synthesis: a hypothesis related to melatonin's primary function and evolution in eukaryotes. *J Pineal Res*. 2013;3:127-138.

## SUPPORTING INFORMATION

Additional supporting information may be found online in the Supporting Information section at the end of the article.

**How to cite this article:** Mandal MK, Suren H, Ward B, Boroujerdi A, Kousik C. Differential roles of melatonin in plant-host resistance and pathogen suppression in cucurbits. *J Pineal Res*. 2018;65:e12505. <https://doi.org/10.1111/jpi.12505>